NFκB decoy complex highly accumulated in the spleen, while the naked NFκB decoy did not highly accumulate in the liver or spleen. The highest accumulation of naked [^{32}P] NFκB decoy was observed in the kidney. Although naked [^{32}P] NFκB decoy rapidly disappeared from the blood circulation, the Fuc-liposome/[^{32}P] NFκB decoy complex maintained a higher blood concentration than the naked [^{32}P] NFκB decoy.

3.3. NPC accumulation of Fuc-liposome/NFκB decoy complex

After intravenous injection of Fuc-liposome/[^{32}P] NFκB decoy complex, the radioactivity in the liver was preferentially recovered from the NPC fraction with the radioactivity ratio of NPC to PC (NPC/PC ratio on a cell-number basis) in the liver being approximately 4.49 (Fig. 2). In contrast, naked [^{32}P] NFκB decoy had an NPC/PC ratio of 0.66 (Fig. 2). The total liver accumulation of Fuc-liposome/[^{32}P] NFκB decoy complex was higher than that of the naked [^{32}P] NFκB decoy.

3.4. Inhibition of Fuc-liposome/NFκB decoy complex liver accumulation by $GdCl_3$ pretreatment

$GdCl_3$ pretreatment inhibits the uptake of Kupffer cells after intravenous injection [23,24]. The hepatic uptake of Fuc-liposome/[^{32}P] NFκB complex was effectively inhibited by $GdCl_3$ pretreatment (Fig. 3). On the other hand, the uptake by spleen and lung was slightly increased by $GdCl_3$ pretreatment.

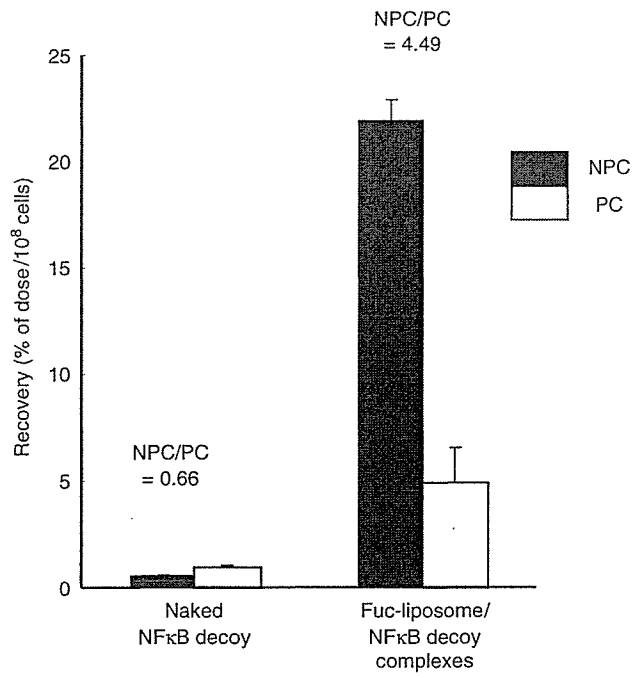

Fig. 2. Intrahepatic distribution of [^{32}P] naked NFκB decoy (A) and Fuc-liposome/[^{32}P] NFκB decoy complex (B) (NFκB decoy 20 μg/mouse) after intravenous injection into mice. [^{32}P] NFκB was complexed with Fuc-liposomes at a charge ratio of 1.0:2.3 (−:+). Radioactivity was determined in NPC (■) and PC (□). Each value represents the mean±S.D. ($n = 4$).

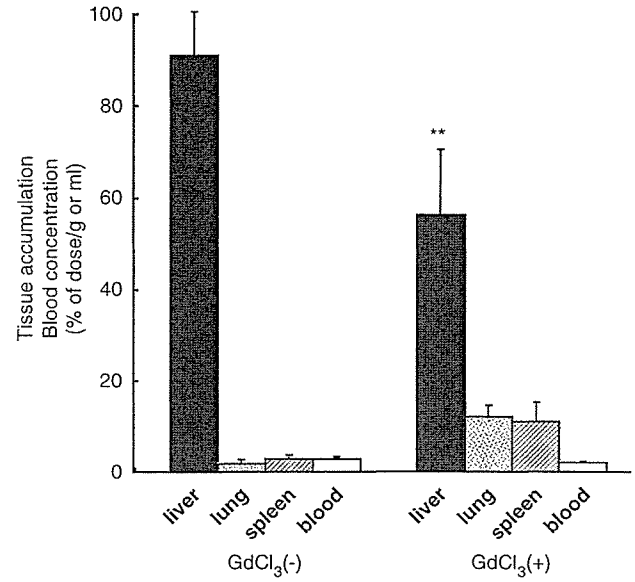

Fig. 3. Tissue accumulation of Fuc-liposome/[^{32}P] NFκB decoy complex (NFκB decoy 20 μg/mouse) after intravenous injection into mice, with or without $GdCl_3$ pretreatment. [^{32}P] NFκB decoy was complexed with Fuc-liposomes at a charge ratio of 1.0:2.3 (−:+). Radioactivity was determined in blood, liver, lung and spleen after 5 min. Each value represents the mean±S.D. ($n = 3$). Significant difference $^{**}P<0.01$.

3.5. Suppression of inflammatory cytokine production by Fuc-liposome/NFκB decoy complexes

To confirm that NFκB complexed with Fuc-liposomes effectively suppressed the production of inflammatory cytokines by Kupffer cells in vivo, the serum concentration of TNFα was measured using ELISA (Fig. 4). Control mice were treated with 5% dextrose after injection of LPS. The serum level of TNFα increased dramatically after LPS treatment as expected, and in vivo Kupffer cell-targeted delivery of NFκB decoy by Fuc-liposomes blocked the increase in the production of TNFα (Fig. 4). On the other hand, intravenously injected naked NFκB decoy and Fuc-liposome/random decoy complexes did not affect the serum level of TNFα (Fig. 4). The same amount of NFκB decoy complexed with Man-liposomes slightly reduced the serum level of TNFα (Fig. 4). After LPS treatment, the serum level of IFNγ (2.57±0.82 ng/ml, $n = 4$), which is also regulated by NFκB, was also significantly reduced by Fuc-liposome complexes (0.246±0.122 ng/ml, $n = 4$) but not by naked NFκB decoy (2.57±1.30 ng/ml, $n = 4$).

3.6. Suppression of liver enzyme production by Fuc-liposome/NFκB decoy complexes

To confirm that NFκB complexed with Fuc-liposomes effectively suppressed liver injury, the serum concentrations

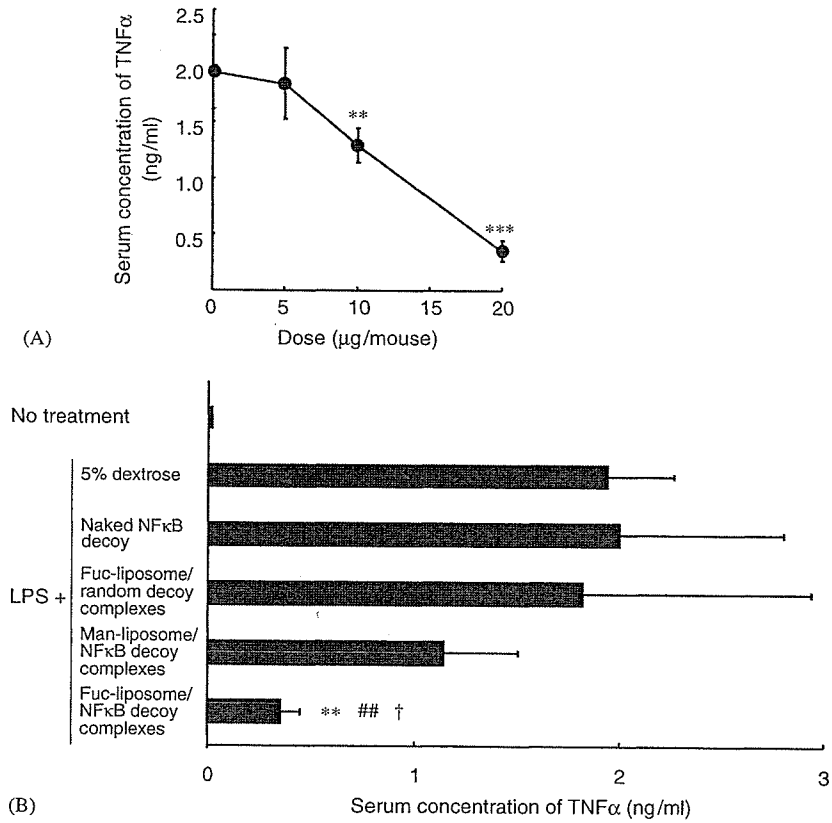

Fig. 4. Inhibitory effect of Fuc-liposome/NFκB decoy complex on the production of TNFα at different doses (A) and comparison with naked NFκB decoy and Fuc-liposome/NFκB decoy complexes (NFκB decoy or random decoy 20 μg/mouse) (B). Serum concentration of TNFα was determined by ELISA. One minute after intravenous administration of LPS, Fuc-liposome/NFκB decoy complexes were intravenously injected into mice. Blood was collected from the vena cava at 1 h. Each value represents the mean ± S.D. ($n = 3-4$). Significant difference $^{***}P<0.001$; $^{**}P<0.01$ v.s. dose of 0 μg of NFκB decoy/mouse in (A), $^{**}P<0.01$ v.s. LPS; $^{\#\#}P<0.01$ v.s. LPS + naked NFκB decoy; $^{\dagger}P<0.05$ v.s. Man-liposome/NFκB decoy complexes in (B).

of ALT and AST were assessed (Fig. 5). Control mice were treated with 5% dextrose after injection of LPS and D-galactosamine. The serum levels of ALT and AST increased dramatically after LPS with D-galactosamine treatment as expected, and in vivo Kupffer cell targeted delivery of NFκB decoy by Fuc-liposomes blocked the increase in the production of ALT and AST (Fig. 5). On the other hand, intravenously injected naked NFκB decoy had no effect on the serum levels of ALT and AST (Fig. 5). Fuc-liposome/random decoy complex also did not reduce the serum level of ALT and AST (data not shown).

3.7. Prevention of NFκB activation by Fuc-liposome/NFκB decoy complexes

In response to inflammatory stimuli, IκB protein degraded and allowed NFκB to translocate into the nucleus to initiate gene expression of inflammatory cytokines. The amount of activated NFκB in the nuclei was measured by EIA to confirm the inhibitory effect of Fuc-liposome complexes on the activation of NFκB. After LPS treatment, the amount of activated NFκB was dramatically increased. However, after injection of Fuc-liposome complexes, the amount of activated NFκB in nuclei did not increase following LPS treatment (Fig. 6).

4. Discussion

Recently, new techniques to inhibit target gene expression using oligonucleotides, such as decoy oligonucleotides, antisense DNA, ribozyme and siRNA, have been developed, and these are expected to be attractive treatments without side effects on genome DNA compared with pDNA. However, oligonucleotides are easily degraded in blood and rapidly metabolized and, therefore, potential carriers have to be developed capable of carrying enough oligonucleotide to produce a therapeutic effect. As far as liver failure is concerned, Kupffer cells, hepatic resident macrophages, play an important role in producing several kinds of systemic cytokines [25,26]. Furthermore, because intravenous injection is a non-invasive method that does not require special techniques, intravenous injectable carrier is desirable in clinical situations. Therefore, the purpose of this study is to develop a Kupffer cell-selective delivery system for NFκB decoy by intravenous injection and to suppress cytokine production.

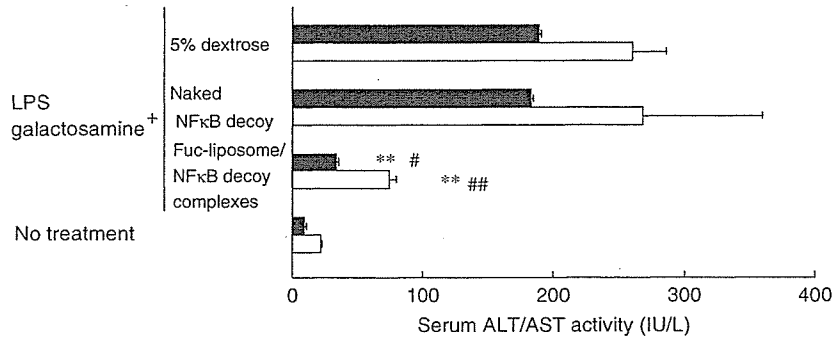

Fig. 5. Inhibitory effect of Fuc-liposome/NFκB decoy complex on liver enzyme injury. One min after intravenous administration of LPS with D-Galactoasmine, Fuc-liposome/NFκB decoy complex or naked NFκB decoy (NFκB decoy 20 μg/mouse) was intravenously injected into mice. Blood was collected from the vena cava at 3 h. Each value represents the mean±S.D. ($n = 4$). Significant difference $^{**}P<0.01$ v.s. + 5% dextrose; $^{\#}P<0.05$; $^{\#\#}P<0.01$ v.s. + naked NFκB decoy.

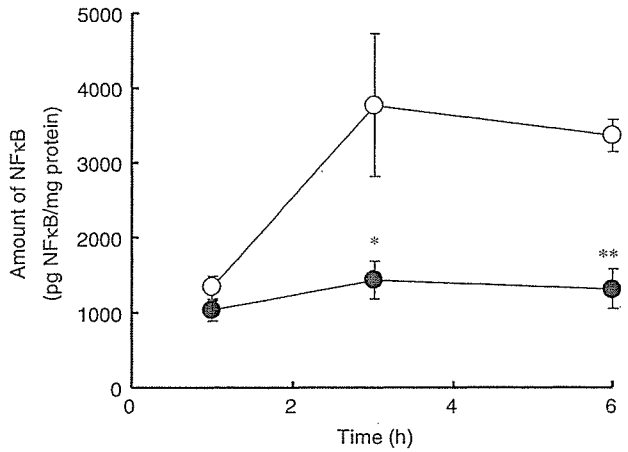

Fig. 6. Inhibitory effect of Fuc-liposome/NFκB decoy complex on NFκB activation in the nuclei. One min after intravenous administration of LPS, Fuc-liposome/NFκB decoy complex (20 μg/mouse) was intravenously injected into mice (●). Control mice were treated with 5% dextrose after injection of LPS (○). Liver was excised from mice at 1, 3 and 6 h. Each value represents the mean±S.D. ($n = 3-4$). Significant difference $^{**}P<0.01$; $^{*}P<0.05$.

In order to investigate Kupffer cell-selective delivery of NFκB decoy using Fuc-liposomes, the tissue accumulation and intrahepatic distribution of Fuc-liposome/[^{32}P] NFκB decoy complexes was examined after intravenous injection (Fig. 1). Rapid and high liver accumulation of Fuc-liposome/[^{32}P] NFκB decoy complexes was observed. Moreover, Fuc-liposome/NFκB decoy complexes were preferentially taken up by NPC (Fig. 2). To confirm the contribution of Kupffer cells to NPC accumulation, the hepatic uptake of Fuc-liposome/NFκB decoy complex was compared with and without $GdCl_3$ pretreatment, because $GdCl_3$ pretreatment, which inhibits the uptake ability of Kupffer cells without any inflammation by other liver cells, was widely used to analyze Kupffer cell function including uptake and cytokines production etc. [23,24]. The liver accumulation was lower with $GdCl_3$ pretreatment than without it (Fig. 3), which strongly supported Fuc-liposome/NFκB decoy complexes being efficiently taken up by Kupffer cells. This uptake characteristic agrees with the results of the uptake of Fuc-BSA [17]. It has been reported that after single injection of $GdCl_3$ Kupffer cells but not spleen macrophage strongly inhibited receptor mediated binding [23]. This may explain the fact that the spleen uptake of NFκB decoy/Fuc-liposome complexes was increased under $GdCl_3$ treatment (Fig. 3).

After intravenous injection, the distribution of a macromolecule is basically decided by its physicochemical properties, including size and charge. The kidney and liver play an important role in the disposition of macromolecules circulating in the blood [27]. Macromolecules with a molecular weight of less than 50,000 (approximately 6 nm in diameter) are susceptible to glomerular filtration and are excreted into the urine [28]. As far as the distribution of NFκB decoy is concerned, although [^{32}P] NFκB decoy rapidly disappeared from the blood, the Fuc-liposome/NFκB decoy complexes circulated for a little longer (Fig. 1). Considering that the molecular weight of NFκB decoy is about 13,000, this result indicates that Fuc-liposome/NFκB decoy complexes escape rapid glomerular filtration and increase the stability of NFκB decoy in the blood.

It is well known that NFκB decoy can be bound by activated NFκB and inhibits the transfer activated NFκB to the nuclei, consequently inhibiting the transcription of NFκB [29]. To determine the inhibitory mechanism of cytokine production by Fuc-liposome/NFκB decoy complexes, the amount of NFκB in the nuclei was measured by EIA. After injection of Fuc-liposome/NFκB decoy complexes, the amount of NFκB in the nuclei was lower than that after only LPS treatment (Fig. 4). This result shows that NFκB decoy delivered by Fuc-liposomes can inhibit the transfer of activated NFκB to nuclei. Moreover, Fuc-liposome/NFκB decoy complexes can inhibit the production of TNFα and IFNγ (Fig. 4), the expression of which is regulated by NFκB. This result also shows that Fuc-liposome/NFκB decoy complexes can suppress the

activation of NFκB. As far as liver injury is concerned, serum ALT and AST levels were measured, because cytokine release from Kupffer cells has a cytotoxic effect on hepatocytes. ALT and AST levels were suppressed by Fuc-liposome/NFκB decoy complexes but not naked NFκB decoy (Fig. 5). This result also shows the Fuc-liposome/NFκB decoy complexes can suppress the activation of NFκB.

In a previous study, we demonstrated that intravenously injected bare cationic liposome/NFκB decoy complexes [22] and Man-liposome/NFκB decoy complexes [30] suppressed LPS-induced TNFα production in mice. Unlike Fuc-liposome complexes, after intravenous injection cationic liposome complexes rapidly and highly accumulated in the lung and then slowly accumulated in the liver (about 60% of dose/g tissue) [22]; therefore, liver accumulation of cationic liposome complexes was lower than that of Fuc-liposome complexes (Fig. 1). This could explain the fact that the production of TNFα could be attenuated by 20 μg NFκB decoy complexed with Fuc-liposomes but not by cationic liposomes (Fig. 4). As far as the characteristics of receptor recognition are concerned, both mannose receptor, which is expressed on sinusoidal endothelial cells and Kupffer cells, and fucose receptor, which is expressed on Kupffer cells, could recognize mannose and fucose. However, in our previous reports, intravenously injected mannosylated bovine serum albumin (BSA) was taken up by sinusoidal endothelial cells compared with Kupffer cells and fucosylated BSA was more selectively taken up Kupffer cells compared with sinusoidal endothelial cells [16,31]. This could explain the fact that 20 μg NFκB decoy complexed with Fuc-liposome more strongly reduced the serum level of TNFα than the same amount of NFκB decoy complexed with Man-liposomes (Fig. 4).

As far as the liver-specific delivery of NFκB decoy is concerned, Yoshida et al. [32] recently demonstrated that NFκB decoy was effectively transferred to Kupffer cells by fusigenic liposomes with hemagglutinating virus of Japan (HVJ liposomes) from the portal vein. Using this method, Ogushi et al. [33] demonstrated that NFκB decoy incorporated in HVJ liposomes effectively suppressed endotoxin-induced fatal liver injury in mice. However, intraportal injection is difficult in clinical situations because it needs a skillful surgical technique and increases the burden on the patient. Although intravenous injection is the simplest method, HVJ liposomes cannot accumulate in the liver following intravenous injection, because HVJ liposomes fuse to cells in a non-specific manner [32]. As a consequence, oligonucleotide is non-specifically delivered by HVJ liposomes to the lung, spleen and kidneys after intravenous injection [32]. In fact, Ogushi et al. [33] achieved a therapeutic effect only by intraportal injection of HVJ liposomes not by intravenous injection. Moreover, because Kupffer cells account for only 15% of the total liver cells [33], non-specific fusion of HVJ liposomes would cause an increase in the dose of NFκB decoy. Furthermore, preparing HVJ liposomes is complicated with irradiation being needed to remove viral toxicity and centrifugation to remove free HVJ [34].

5. Conclusion

In this study, novel Fuc-liposomes can be used as Kupffer cell-selective oligonucleotide carriers through recognition by the fucose receptors on Kupffer cells. Intravenously injected Fuc-liposome/NFκB decoy complexes effectively suppress LPS-induced TNFα and IFNγ production by suppression of NFκB transcription. Liver injury following to the cytokines production was also prevented Fuc-liposome/NFκB decoy complexes. Fuc-liposome/NFκB decoy complexes will prove to be a useful therapeutic tool for treating cytokine-related fatal inflammatory liver disease following administration by intravenous injection.

Acknowledgements

This work was supported in part by The Research Foundation for Pharmaceutical Sciences, Grants-in-Aid for Scientific Research from the Ministry of Education, Culture, Sports, Science, and Technology of Japan, and by Health and labor Sciences Research Grants for Research on Advanced Medical Technology from the Ministry of Health, Labor and Welfare of Japan, and The Research Foundation for Pharmaceutical Sciences and by Radioisotope Research Center of Kyoto University.

References

[1] Morrison DC, Ryan JL. Endotoxins and disease mechanisms. Annu Rev Med 1987;38:417–32.
[2] Ponnappa BC, Dey I, Tu GC, Zhou F, Aini M, Cao QN, et al. In vivo delivery of antisense oligonucleotides in pH-sensitive liposomes inhibits lipopolysaccharide-induced production of tumor necrosis factor in rats. J Pharmacol Exp Ther 2001;297:1129–36.
[3] Pahl HL. Activations and target genes of Rel/NF-κB transcription factors. Oncogene 1999;18:6853–66.
[4] Handa O, Naito Y, Takagi T, Shimozawa M, Kokura S, Yoshida N, et al. Tumor necrosis factor-alpha-induced cytokine-induced neutrophil chemoattractant-1 (CINC-1) production by rat gastric epithelial cells: role of reactive oxygen species and nuclear factor-κB. J Pharmacol Exp Ther 2004;309:670–6.
[5] Wrighton CJ, Hofer-Warbinek R, Moll T, Eytner R, Bach FH, de Martin R. Inhibition of endothelial cell activation by adenovirus-mediated expression of IκBa, an inhibitor of the transcription factor NF-κB. J Exp Med 1996;183:1013–22.
[6] Foxwell B, Browne K, Bondeson J, Clarke C, de Martin R, Brennan F, et al. Efficient adenoviral infection with IκBa reveals that macrophage TNFα production in rheumatoid arthritis is NF-κB dependent. Proc Natl Acad Sci USA 1998;95:8211–5.
[7] Bielinska A, Shivdasani RA, Zhang LQ, Nabel GJ. Regulation of gene expression with double-stranded phosphorothioate oligonucleotides. Science 1990;250:997–1000.
[8] Morishita R, Higaki J, Tomita N, Ogihara T. Application of transcription factor "decoy" strategy as means of gene therapy and study of gene expression in cardiovascular disease. Circ Res 1998;82:1023–8.
[9] Morishita R, Sugimoto T, Aoki M, Kida I, Tomita N, Moriguchi A, et al. In vivo transduction of cis element decoy against nuclear

factor-κB binding siteprevents myocardial infraction. Nat Med 1997; 3:894–9.
[10] Griesenbach U, Scheid P, Hillery E, de Martin R, Huang L, Geddes DM, et al. Anti-inflammatory gene therapy directed at the airway epithelium. Gene Ther 2000;7:306–13.
[11] Higuchi Y, Kawakami S, Nishikawa M, Yamashita F, Hashida M. Intracellular distribution of NFκB decoy and its inhibitory effect on TNFα production by LPS stimulated RAW 264.7 cells. J Control Release 2005;107:373–82.
[12] Kawakami S, Yamashita F, Nishida K, Nakamura J, Hashida M. Glycosylated cationic liposomes for cell-selective gene delivery. Crit Rev Ther Drug Carrier Syst 2002;19:171–90.
[13] Kawakami S, Sato A, Nishikawa M, Yamashita F, Hashida M. Mannose receptor-mediated gene transfer into macrophages using novel mannosylated cationic liposomes. Gene Ther 2000;7:292–9.
[14] Yamada M, Nishikawa M, Kawakami S, Hattori Y, Nakano T, Yamashita F, et al. Tissue and intrahepatic distribution and subcellular localization of a mannosylated lipoplex after intravenous administration in mice. J Control Release 2004;98:157–67.
[15] Hattori Y, Kawakami S, Suzuki S, Yamashita F, Hashida M. Enhancement of immune responses by DNA vaccination through targeted gene delivery using mannosylated cationic liposome formulations following intravenous administration in mice. Biochem Biophys Res Commun 2004;317:992–9.
[16] Opanasopit P, Nishikawa M, Yamashita F, Takakura Y, Hashida M. Pharmacokinetic analysis of lectin-dependent biodistribution of fucosylated bovine serum albumin: a possible carrier for Kupffer cells. J Drug Target 2001;9:341–51.
[17] Kuiper J, Brouwer A, Knook DL, van Berkel TJC. Kupffer and sinusoidal endothelial cells. In: Arias IM, Boyer JL, Fausto N, Jakoby WB, Schachter DA, Shafritz DA, editors. The liver: biology and pathobiology. 3rd ed. New York: Raven Press; 2001. p. 791–818.
[18] Kawakami S, Wong J, Sato A, Hattori Y, Yamashita F, Hashida M. Biodistribution characteristics of mannosylated, fucosylated, and galactosylated liposomes in mice. Biochim Biophys Acta 2000;1524: 258–65.
[19] Hattori Y, Suzuki S, Kawakami S, Yamashita F, Hashida M. The role of dioleoylphosphatidylethanolamine (DOPE) in targeted gene delivery with mannosylated cationic liposomes via intravenous route. J Control Release 2005;108:484–95.
[20] Yeeprae W, Kawakami S, Higuchi Y, Yamashita F, Hashida M. Biodistribution characteristics of mannosylated and fucosylated O/W emulsions in mice. J Drug Target 2005;13:479–87.
[21] Yang JP, Huang L. Overcoming the inhibitory effect of serum on lipofection by increasing the charge ratio of cationic liposome to DNA. Gene Ther 1997;4:950–60.
[22] Higuchi Y, Kawakami S, Oka M, Yamashita F, Hashida M. Suppression of TNFα production in LPS induced liver failure mice after intravenous injection of cationic liposome/NFκB decoy complex. Pharmazie 2006;61:144–7.
[23] Hardonk MJ, Dijkhuis FW, Hulstaert CE, Koudstaal J. Heterogeneity of rat liver and spleen macrophages in gadolinium chloride-induced elimination and repopulation. J Leukoc Biol 1992;52:296–302.
[24] Rüttinger D, Vollmar B, Wanner GA, Messmer K. In vivo assessment of hepatic alterations following gadolinium chloride-induced Kupffer cell blockade. J Hepatol 1996;25:960–7.
[25] Mas A, Rodés J. Fulminant hepatic failure. Lancet 1997;349:1081–5.
[26] Roland N, Wade J, Davalos M, Wendon J, Philpott-Howars J, Williams R. The system inflammatory response syndrome in acute liver failure. Hepatology 2000;32:734–9.
[27] Sands H, Gorey-Feret LJ, Cocuzza AJ, Hobbs FW, Chidester D, Trainor GL. Biodistribution and metabolism of internally ^{3}H-labeled oligonucleotides. I. Comparison of a phosphodiester and a phosphorothioate. Mol Pharmacol 1994;45:932–43.
[28] Brenner BM, Hostetter TH, Humes HD. Glomerular permselectivity: barrier function based on discrimination of molecular size and charge. Am J Physiol 1978;234:F455–60.
[29] Dzau VJ, Mann MJ, Morishita R, Kaneda Y. Fusigenic viral liposome for gene therapy in cardiovascular diseases. Proc Natl Acad Sci USA 1996;93:11421–5.
[30] Higuchi Y, Kawakami S, Oka M, Yabe Y, Yamashita F, Hashida M. Intravenous administration of mannosylated cationic liposome/$NF_{\kappa}B$ decoy complexes effectively prevent LPS-induced cytokine production in a murine liver model. FEBS Lett 2006;580:3706–14.
[31] Ogawara K, Hasegawa S, Nishikawa M, Hashida M. Pharmacokinetic evaluation of mannosylated bovine serum albumin as a liver cell-specific carrier: quantitative comparison with other hepatoropic ligands. J Drug Target 1999;6:349–60.
[32] Yoshida M, Yamamoto N, Uehara T, Terao R, Nitta R, Harada N, et al. Kupffer cell targeting by intraportal injection of the HVJ cationic liposome. Eur Surg Res 2002;34:251–9.
[33] Ogushi I, Iimuro Y, Seki E, Son G, Hirano T, Hada T, et al. Nuclear factor κB decoy oligonucleotides prevent endotoxin-induced fatal liver failure in a murine model. Hepatology 2003;38:335–44.
[34] Hirano T, Fujimoto J, Ueki T, Yamamoto H, Iwasaki T, Morisita R, et al. Persistent gene expression in rat liver in vivo by repetitive transfections using HVJ-liposome. Gene Ther 1998;5:459–64.

Available online at www.sciencedirect.com
ScienceDirect
Biomaterials 28 (2007) 1434–1442
Biomaterials
www.elsevier.com/locate/biomaterials

Small interfering RNA delivery to the liver by intravenous administration of galactosylated cationic liposomes in mice

Ayumi Sato[a], Motoki Takagi[a], Akira Shimamoto[a], Shigeru Kawakami[b], Mitsuru Hashida[b,*]

[a]*GeneCare Research Institute Co. Ltd., 200 Kajiwara, Kamakura, Kanagawa 247-0063, Japan*
[b]*Department of Drug Delivery Research, Graduate School of Pharmaceutical Sciences, Kyoto University, Sakyo-ku, Kyoto 606-8501, Japan*

Received 20 September 2006; accepted 7 November 2006
Available online 4 December 2006

Abstract

Although small interfering RNA (siRNA) is a potentially useful therapeutic approach to silence the targeted gene of a particular disease, its use is limited by its stability in vivo. For the liver parenchymal cell (PC)-selective delivery of siRNA, siRNA was complexed with galactosylated cationic liposomes. Galactosylated liposomes/siRNA complex exhibited a higher stability than naked siRNA in plasma. After intravenous administration of a galactosylated liposomes/siRNA complex, the siRNA did not undergo nuclease digestion and urinary excretion and was delivered efficiently to the liver and was detected in PC rather than liver non-parenchymal cells (NPC). Endogenous gene (Ubc13 gene) expression in the liver was inhibited by 80% when Ubc13–siRNA complexed with galactosylated liposomes was administered to mice at a dose of 0.29 nmol/g. In contrast, the bare cationic liposomes did not induce any silencing effect on Ubc13 gene expression. These results indicated that galactosylated liposomes/siRNA complex could induce gene silencing of endogenous hepatic gene expression. The interferon responses by galactosylated liposomes/siRNA complex were controlled by optimization of the sequence of siRNA. Also no liver toxicity due to galactosylated liposomes/siRNA complex was observed under any of the conditions tested. In conclusion, we demonstrated the hepatocyte-selective gene silencing by galactosylated liposomes following intravenous administration.

Keywords: Gene therapy; Liver; Liposome; Gene transfer

1. Introduction

RNA interference (RNAi) is induced by 21–25 nucleotide, double-stranded small interfering RNA (siRNA), which is incorporated into the RNAi-induced silencing complex (RISC) and is a guide for cleavage of the complementary target mRNA in the cytoplasm [1]. For therapeutic application, siRNA technology promises greater advantages over drugs currently on the market by offering new types of drugs that are easy to design and have a very high target selectivity, inhibiting a specific gene expression in the cytoplasm, and an expected low toxicity due to metabolism to natural nucleotide components by the endogenous cell systems [1–5]. However, siRNA therapeutics is hindered by the poor intracellular uptake and limited blood stability of siRNA and the current delivery methods to the target cells in vivo. When siRNA is administered in blood, it is readily digested by nuclease and eliminated from the renal glomeruli before reaching the diseased tissues. In order to achieve the therapeutic effect of siRNA at the target site, therefore, it is important to enhance the stability of siRNA in the blood circulation and to allow targeted delivery to the diseased area.

As far as in vivo selective gene delivery to hepatocytes is concerned, galactose has been shown to be a promising targeting ligand to hepatocytes (liver PCs) because the cells possess a large number of asialoglycoprotein receptors that recognize the galactose units on the oligosaccharide chains of glycoproteins or on the chemically synthesized galactosylated carriers [6]. In a series of investigations, we have studied liposomal systems to deliver plasmid DNA to hepatocytes in vivo and developed novel galactosylated cationic liposomes, including cationic charge linkers for

*Corresponding author. Tel.: +81 75 753 4525; fax: +81 75 753 4575.
E-mail address: hashidam@pharm.kyoto-u.ac.jp (M. Hashida).

0142-9612/$ - see front matter © 2006 Elsevier Ltd. All rights reserved.
doi:10.1016/j.biomaterials.2006.11.010

anionic compound binding and galactose moieties as a targetable ligand for PC. The galactosylated cationic liposomes are composed of galactosylated cholesterol derivatives, cholesten-5-yloxy-*N*-(4-((1-imino-2-D-thiogalactosylethyl)amino)alkyl)formamide (Gal-C4-Chol) and a neutral lipid. Based on the optimization of the physicochemical properties of the galactosylated liposomes/plasmid DNA complexes [7–10], we have succeeded in developing a hepatocyte-selective gene targeting system. Ma et al. [11] have reported that cationic liposomes enhance siRNA-mediated interferon (IFN) responses by the activation of STAT1 in mice. In contrast, naked siRNA did not induce the IFN responses. Recently, Zhang and Wang have reported that the siRNA of hepatitis C is a novel strategy for the treatment of this disease in vitro [12,13]. Since IFN can be used for the treatment of virus hepatitis, these observations prompted us to investigate whether a galactosylated liposomes/siRNA complex could achieve both gene silencing in hepatocytes and IFN induction after intravenous administration.

In the present study, siRNA delivery to the liver by intravenous administration of galactosylated liposomes was examined. Results are compared with naked siRNA (conventional injection or hydrodynamic injection) and cationic liposomes/siRNA complex.

2. Materials and methods

2.1. Materials

Dioleoylphosphatidylethanolamine (DOPE), 3β[*N*-(*N'*,*N'*-dimethylaminoethane)carbomyl]cholesterol (DC-Chol), L-α-phosphatidylcholine, hydrogenated from chicken egg (Egg PC) and 1,2-dioleoyl-*sn*-glycero-3-phosphocholine (DOPC) were purchased from Avanti Polar-Lipids Inc. (Alabaster, AL). The preparation of Gal-C4-Chol has been described previously [14]. siRNAs (21 mer) with 3′-dTdT overhangs were chemically synthesized by Nippon EGT Co. Ltd. (Toyama, Japan). The siRNA sequences are shown in Table 1. The Ubc13 siRNA modified with Alexa Fluor 546 or fluorescein at the 3′ termini of the sense strand was synthesized by QIAGEN K.K. (Tokyo, Japan).

2.2. Preparation of liposomes

A mixture of Gal-C4-Chol and DOPE with a molar ratio of 3:2 was dissolved in chloroform, vacuum-desiccated, and resuspended in sterile 5% dextrose solution. The suspension was sonicated and the resulting liposomes were extruded 10 times through double-stacked 100 nm polycarbonate membrane filters. Cationic liposomes and siRNA was complexed at a charge ratio (−:+) of 1.0:2.3 for cell-selective delivery [7]. The particle size and zeta potential of the liposomes were measured using a Nano ZS apparatus (Malvern Instruments Ltd., Malvern, WR, UK). All other liposomes, Gal-C4-Chol, cholesterol, and DOPE (molar ratio = 1:1:1), Gal-C4-Chol and Egg PC (molar ratio = 3:2) and Gal-C4-Chol and DOPC (molar ratio = 3:2) were prepared by a similar procedure.

2.3. Stability of galactosylated liposomes/siRNA complex in mouse plasma

For siRNA stability in blood plasma, a solution (30 μl) of 150 pmol siRNA (Alexa Fluor 546-labeled siRNA: no labeled siRNA = 1:4) complexed with the galactosylated liposomes (Gal-C4-Chol/DOPE liposomes) was mixed with 270 μl fresh mouse plasma to give a final plasma concentration of 90%. After incubation at 37 °C for specific time periods, aliquots (20 μl) were collected and mixed with 10 μl 9% sodium dodecyl sulfate solution. The siRNAs were extracted from the reaction mixtures with phenol/chloroform/isoamyl alcohol (25:24:1). The siRNAs were electrophoresed on 4–20% polyacrylamide gel (Tefco Inc., Tokyo, Japan) and visualized with a fluorescence image analyzer, FMBIO II (Hitachi Software Engineering Co. Ltd., Tokyo, Japan).

2.4. Stability of galactosylated liposomes/siRNA complex in vivo

The animal experiments in the present study were approved by the Animal Research Committee of the GeneCare Research Institute Co. Ltd. Male ICR mice (age 5 weeks) were purchased from CLEA Japan Inc. (Tokyo, Japan). For the in vivo stability study of siRNA, Alexa Fluor 546-labeled siRNA and unlabeled siRNA were mixed in a 1:4 ratio. The galactosylated liposomes (Gal-C4-Chol/DOPE liposomes)/siRNA complex solution was administered intravenously (0.1 nmol siRNA/10 μl/g) and blood samples were collected from each mouse. Then 20 μl of each blood sample was added to 10 μl 9% sodium dodecyl sulfate solution. The siRNAs in the blood samples were extracted and electrophoresed by the procedures described above.

2.5. Biodistribution of galactosylated liposomes/siRNA complex in mice

The galactosylated liposomes (Gal-C4-Chol/DOPE liposomes) and fluorescein-labeled siRNA complex solution was injected intravenously into mice (0.1 nmol siRNA/10 μl/g). At 5 and 60 min following administration, the organs were harvested and rinsed with saline. The fluorescein-labeled siRNA in the organs was visualized in a fluorescence image analyzer, FMBIO II.

2.6. Detection of siRNA in liver cells

The liposomes and fluorescein-labeled siRNA complex solution was injected intravenously into mice (0.1 nmol siRNA/10 μl/g). At 48 h post-injection of the liposomes/siRNA complex, the liver was removed rinsed with saline, frozen in liquid nitrogen and mounted for cryostat sectioning. Slides were viewed under a fluorescence microscope.

Table 1
Sequence of siRNAs

siRNA	Sequence of sense strand
Ubc13–siRNA	5′-GUACGUUUCAUGACCAAAA-dTdT-3′
Non-specific control siRNA (NS-siRNA)	5′-UUCUCCGAACGUGUCACGU-dTdT-3′
siRNA1	5′-GUUCAGACCACUUCAGCUU-dTdT-3′
siRNA2	5′-GCUUGAAACUAUUAACGUA-dTdT-3′

2.7. Gene silencing effect in various organs

Liposomes and Ubc13 siRNA complex solution were injected intraportally or intravenously into mice at a normal pressure (0.18 nmol siRNA/18 μl/g). As for the hydrodynamic injection, Ubc13 siRNA were injected intravenously at a volume of 1.6 ml siRNA solution [15–17]. At 48 h following administration, the organs were removed and rinsed with saline. The total RNAs were extracted from the organs using an RNeasy Mini Kit (Qiagen) according to the manufacturer's protocol. RT-PCR analyses were carried out using an ABI Prism 7000 Sequence Detection System and Taqman probes and primers (Applied Biosystems, Foster City, CA). The glyceraldehyde-3-phosphate dehydrogenase gene (GAPDH) was used as the standard.

2.8. Measurement of IFN, aspartate aminotransferase (AST) and alanine aminotransferase (ALT) in mouse blood

Groups of three mice were intravenously injected with galactosylated liposomes (Gal-C4-Chol/DOPE liposomes)/siRNA (0.18 nmol siRNA/g) complex. At 5 h following the administration, blood samples were collected and the IFN-α and IFN-γ levels measured by ELISA. Mouse IFN-α and IFN-γ ELISA kits were purchased from PBL Biomedical Laboratories (Piscataway, NJ) and GE Healthcare Bio-Sciences Co. (Piscataway, NJ), respectively. The measurements were performed according to the manufacturer's instructions.

For detection of AST and ALT, mouse blood samples were collected at 5 and 20 h following administration. The aminotransferase activities were measured using a Transaminase CII-Test Wako kit (Wako Pure Chemical Industries Ltd., Tokyo, Japan) according to manufacturer's instructions.

3. Results

3.1. Physicochemical properties of galactosylated liposomes/siRNA complex

The particle sizes of the galactosylated liposomes were 50.1 ± 3.6 nm and the zeta potentials were 47.9 ± 0.7 mV (Table 2). Also, the particle sizes of the galactosylated liposomes complexed with siRNA were 75.3 ± 5.8 nm and the zeta potentials were 35.8 ± 1.8 mV. The particle sizes of the galactosylated liposomes/siRNA complex were larger and the zeta potentials were lower than those of the galactosylated liposomes, suggesting that the galactosylated liposomes and siRNA form complexes by their electrostatic interaction.

3.2. Stability of siRNA in mouse plasma

Naked siRNA underwent almost 90% digestion by nuclease within 3 h at 37 °C (Fig. 1). Under the same conditions, the siRNA complexed with galactosylated liposomes remained intact at 30 h. This showed that the galactosylated liposomes conferred a highly protective effect against nuclease as far as siRNA was concerned. Also, this result indicated that the ionic interaction between galactosylated liposomes and siRNA is unaffected by various ionic component, i.e. lipids, proteins, and polysaccharides in plasma.

3.3. Delivery of galactosylated liposomes/siRNA complex to liver

Fig. 2 shows the amount of intact siRNA in the blood circulation after intravenous administration. Naked siRNA was eliminated from the blood within 5 min and excreted in urine. In contrast, the galactosylated liposomes prolonged the circulation of siRNA in the mouse bloodstream compared with naked siRNA. The siRNA was detected in the bloodstream but not in the urine 60 min following injection. This result suggests that the galactosylated liposomes/siRNA complex is not digested by nuclease and eliminated via the renal glomeruli. Furthermore, the complex might be slowly distributed in some organs instead of remaining in the circulating blood.

Next, we investigated the biodistribution of siRNA in the heart, lung, liver, spleen and kidney at 5 and 60 min after administration of the galactosylated liposomes/siRNA complex to mice. The siRNA was detected in the liver, lung and kidney compared with untreated mice at 5 min (Fig. 3). Despite elimination of siRNA from the bloodstream at 60 min, the siRNA remained in the liver and lung. These results show that the siRNA disappearing from the bloodstream is delivered to the liver by galactosylated liposomes formulations.

3.4. Cellular localization of siRNA in liver

Fig. 4 shows images of frozen sections of livers under fluorescence microscopy. In the galactosylated liposomes (Gal-C4-Chol/DOPE)/siRNA complex-injected mice, fluorescein-labeled siRNA was detected abundantly in liver cells and the fluorescence intensity was higher than that in the mice injected with cationic liposomes (DC-Chol/DOPE)/siRNA complex. In construct, there was hardly any siRNA in liver cells when cationic liposomes/siRNA complex was used. Considering that hepatocytes account for almost 80% of the total liver volume by PC, these results indicate that galactosylated liposomes/siRNA complex is incorporated efficiently into PC by the galactose ligand of galactosylated liposomes.

Table 2
Particle size and zeta potential of galactosylated liposomes and its complex

Formulations	Particle size (nm)	ζ potential (mV)
Galactosylated liposomes (Gal-C4-Chol/DOPE)	50.1 ± 3.6	47.9 ± 0.7
Galactosylated liposomes/siRNA complex	75.3 ± 5.8	35.3 ± 1.8

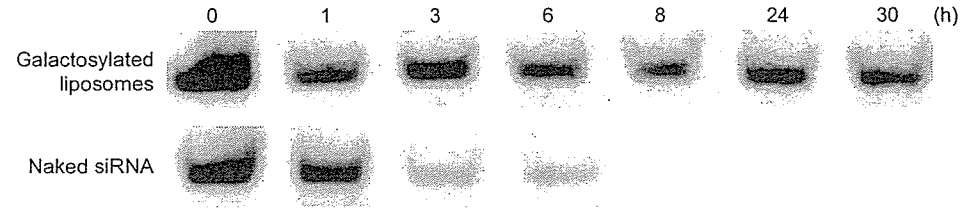

Fig. 1. Stability of galactosylated liposomes/siRNA complex in mouse plasma. Alexa fluor 546-labeled siRNA and unlabeled siRNA mixture (1:4 mol/mol) was complexed with galactosylated liposomes (Gal-C4-Chol/DOPE) and incubated in 90% plasma at 37 °C for 1, 3, 6, 8, 24, and 30 h. The remaining siRNAs were separated by gel electrophoresis and fluorescence labeled siRNAs were detected by image analysis. Naked siRNA was used as a negative control.

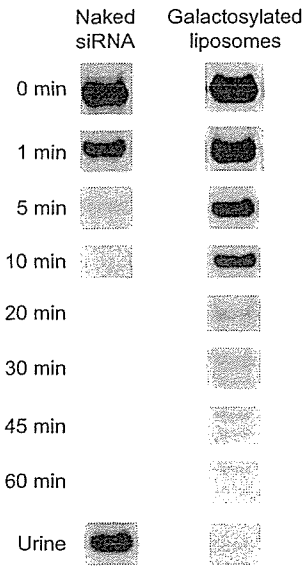

Fig. 2. Stability of siRNA complexed with galactosylated liposomes in blood circulation after intravenous administration in mice. siRNA (Alexa fluor 546-siRNA and unlabeled siRNA = 1:4) complexed with galactosylated liposomes (Gal-C4-Chol/DOPE) was administered to mice intravenously. A total of 40 μl of blood and urine was collected at each time point (urine: 60 min) and the remaining siRNAs were determined by gel electrophoresis and image analysis. Naked siRNA was used as a negative control.

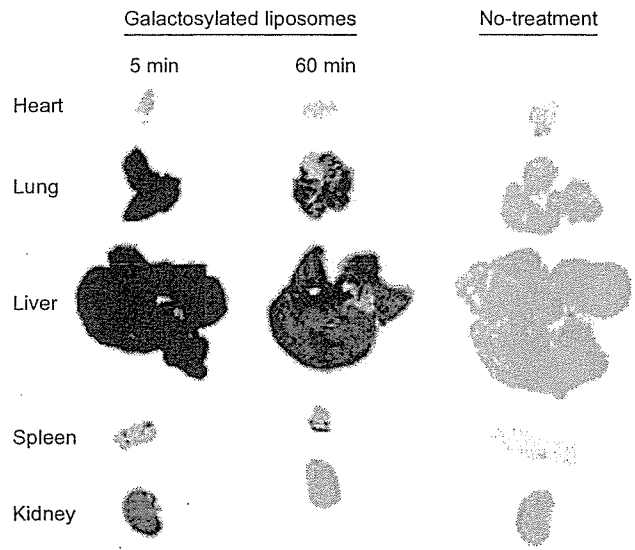

Fig. 3. Biodistribution characteristics of siRNA in tissues after intravenous administration of galactosylated liposomes/fluorescein-labeled siRNA complex in mice. Fluorescein-labeled siRNA complexed with Gal-C4-Chol/DOPE liposomes was administered to mice intravenously. At 5 and 60 min following administration, mice were sacrificed and lung, liver, kidney, spleen and heart were collected. The remaining siRNAs in organs were detected by image analysis. The control is organs from an untreated mouse.

3.5. Silencing of endogenous gene expression in liver

Since siRNA was delivered to liver by galactosylated liposomes after systemic injection into mice, we examined the ability of the siRNA to silence endogenous gene expression in liver. We used the siRNA corresponding Ubc13 gene, which is known to be expressed in various organs constitutively and ubiquitously, and confirmed that the Ubc13 gene is expressed in the mouse lung, liver, kidney, spleen and heart using RT-PCR (data not shown). The Ubc13–siRNA had the ability to suppress 80% of Ubc13 gene expression in HepG2 cells, human hepatic carcinoma, at 1 nm under the culture conditions used (data not shown).

To investigate if Ubc13–siRNA suppresses the expression of Ubc13 mRNA in liver, we administered Ubc13–siRNA into the portal vein of mice using galactosylated liposomes (Gal-C4-Chol/DOPE liposomes) or cationic liposomes (DC-Chol/DOPE liposomes). Although, the silencing effect of the Ubc13 gene expression in liver was observed with each complex after intraportal administration (Fig. 5A), the galactosylated liposomes/siRNA complex exhibited greater suppression of the expression of Ubc13 gene. The in vivo RNAi activity of the Ubc13–siRNA was validated by this result.

The gene suppression effects were also compared with those following hydrodynamic injection [15–17] of Ubc13–siRNA. After intravenous administration, the galactosylated liposomes/Ubc13–siRNA complex effectively suppressed the expression of Ubc13 gene in liver and lung as compared with hydrodynamic injection at 48 h after the injections (Fig. 5B). Notably, the Ubc13 gene expression in liver was suppressed by more than 60% with galactosylated liposomes while in the case of the cationic liposomes complex, no RNAi effects were observed in any organs. These results indicated that galactosylated

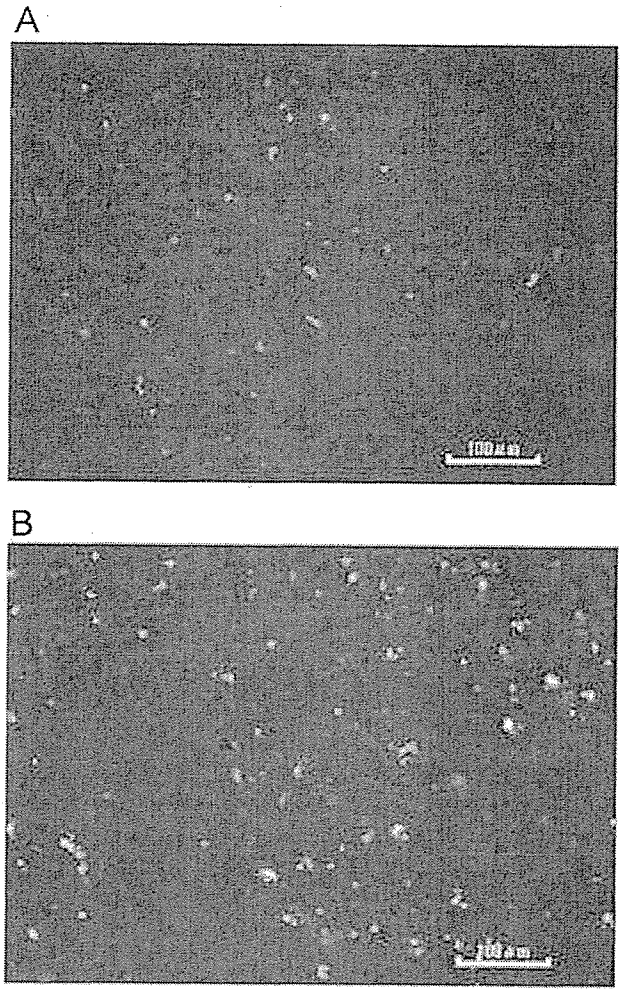

Fig. 4. Cellular localization of siRNA in liver after intravenous administration of galactosylated liposomes/fluorescein-labeled siRNA complex in mice. Fluorescein-labeled siRNA was complexed with cationic liposomes (A) or galactosylated liposomes (B). At 48 h after administration, the livers were removed and mounted for cryostat sectioning. Slides were viewed under a fluorescence microscope.

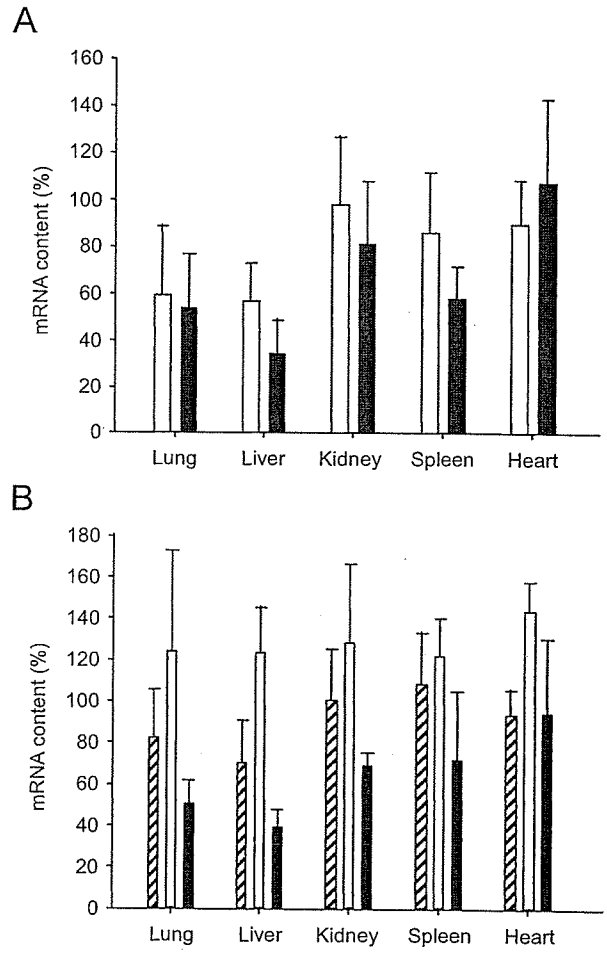

Fig. 5. Suppression of gene expression by galactosylated liposomes/siRNA complex in various organs in mice. Ubc13–siRNA complexed with cationic liposomes (white bar) or galactosylated liposomes (black bar) was injected intraportally (A) or intravenously (B) into mice. Also, Ubc13–siRNA was administered by the hydrodynamic injection method (hatched bar). At 48 h after administration, lung, liver, kidney, spleen and heart were collected. The total RNAs were extracted from the organs and subjected to RT-PCR analysis. Ubc13 mRNA levels in mice given injections of NS-siRNA complexed with respective liposomes, were taken as 100%. Groups of three mice were used and their average expressions of Ubc13 gene are illustrated.

liposomes have a greater potential as a hepatic targeting delivery carrier for siRNA even following intravenous administration.

3.6. Effect of siRNA dose and lipid composition of galactosylated liposomes on gene silencing in liver

We showed that galactosylated liposomes/Ubc13–siRNA complex induces silencing of Ubc13 gene expression in a dose-dependent manner. When 0.1 nmol/g siRNA was administered to mice, no silencing effect was observed (Fig. 6A). However, suppression of Ubc13 gene expression in liver occurred at over 0.18 nmol/g and suppression was observed in other organs at 0.29 and 0.36 nmol/g. The most liver-selective silencing effects were obtained at 0.18 nmol/g. Also, the silencing effect in liver by injection of 0.36 nmol/g siRNA was not greater than that using 0.29 nmol/g. These results showed that the range of siRNA dose-dependence is from 0.18 to 0.36 nmol/g when galactosylated liposomes are used.

To evaluate the lipid composition of galactosylated liposomes, we prepared galactosylated liposomes with Gal-C4-Chol and some neutral lipids, cholesterol, Egg PC and DOPC instead of DOPE. Except for Gal-C4-Chol/Egg PC, these liposomes complexed with siRNA at a charge ratio (−:+) of 1.0:2.3, and Gal-C4-Chol/Egg PC liposomes were prepared at a charge ratio (−:+) of 1.0:1.5. All galactosylated liposomes successfully induced gene silencing of Ubc13 in liver by more than 50% when 0.18 nmol/g siRNA was systemically administered to mice (Fig. 6B). Among the galactosylated liposomes tested, Gal-C4-Chol/DOPE

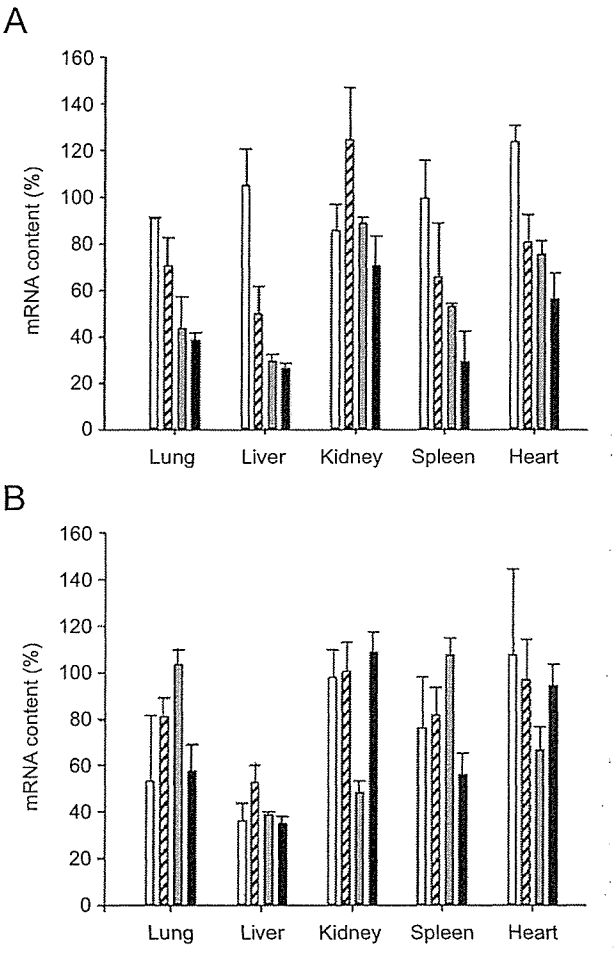

Fig. 6. Effect of siRNA dose (A) and lipid composition of galactosylated liposomes (B) on gene silencing in mice. Galactosylated liposomes (Gal-C4-Chol/DOPE)/Ubc13–siRNA complex was intravenous injected into mice ($N = 3$) at an siRNA dose of 0.10 (white bar), 0.18 (hatched bar), 0.29 (gray bar), or 0.36 (black bar) nmol/g. Ubc13–siRNA complexed with Gal-C4-Chol/DOPE liposomes (white bar), Gal-C4-Chol/cholesterol/DOPE liposomes (hatched bar), Gal-C4-Chol/EggPC liposomes (gray bar) or Gal-C4-Chol/DOPC liposomes (black bar) was intravenous injected into mice ($N = 3$) (B). At 48 h after intravenous administration, organs were collected and subjected to RT-PCR analysis. Ubc13 mRNA levels of mice injected with NS-siRNA complexed with respective liposomes were taken as 100%.

liposomes were the most effective and liver-selective. The silencing effect produced by Gal-C4-Chol/cholesterol/DOPE liposomes in liver was less than that produced by Gal-C4-Chol/DOPE liposomes. These results provide the evidence that Gal-C4-Chol is the most effective means of producing gene silencing with galactosylated liposomes in the liver.

3.7. Immune responses in liver by galactosylated liposomes/siRNA complex

Recent investigations have shown that cationic liposomes/siRNA complex induces IFN responses in mice [11,18–20]. To determine the IFN response by galactosylated liposomes/siRNA complex, we measured the induction level of IFN-α and IFN-γ as type I and type II IFN responses by ELISA. Galactosylated liposomes (Gal-C4-Chol/DOPE liposomes) were complexed with three kinds of siRNAs (NS-siRNA, siRNA1 and siRNA2, shown in Table 1) and injected intravenously into mice. As shown in Fig. 7, the galactosylated liposomes/siRNA complexes and galactosylated liposomes alone, except for siRNA1, failed to induce IFN-α and IFN-γ at 5 h after administration. In contrast, galactosylated liposomes/siRNA1 complex induced a higher level of IFN-α and, especially IFN-γ, compared with galactosylated liposomes/NS-siRNA complex and siRNA2 complex. It has been reported that the immune responses by siRNA are dependent on the sequence of the siRNA [21–23]. These results suggested that IFN responses are not caused by galactosylated liposomes and depend on the siRNA sequence.

The galactosylated liposomes/siRNA complex did not increase ALT and AST levels in mouse serum compared with the levels in untreated mice (Fig. 8). These results indicate that administration of galactosylated liposomes/siRNA complexes do not induce hepatitis in mice even when galactosylated liposomes/siRNA1 complex is injected.

4. Discussion

In this study, we showed that siRNA could be delivered to PC by carrying out experiments involving biodistribution and cellular localization in the liver with galactosylated liposomes (Figs. 3 and 4). Furthermore, we confirmed that endogenous hepatic gene (Ubc13 gene) mRNA is markedly reduced in liver by more than 60% with the galactosylated liposomes/siRNA (Ubc13–siRNA) complex (Figs. 5 and 6). Considering that PC account for about 80% of the total number of liver cells, it is suggested that Ubc13 mRNA in PC is degraded by galactosylated liposomes/siRNA complex. All of these data provide evidence that the inhibition of endogenous gene expression could be accompanied by an efficient uptake of siRNA by PC in liver.

To date, there has been little published information about formulations for the in vivo targeted delivery of siRNA and/or oligonucleotides. In order to optimize the in vivo delivery of siRNA by galactosylated liposomes, the characteristics of galactosylated liposomes as an siRNA delivery system were evaluated based on (i) the route of administration (intraportal vs. intravenous), (ii) the dose of siRNA, and (iii) the composition of neutral helper lipid. Interestingly, an RNAi effect in liver by galactosylated liposomes/siRNA complexes was observed irrespective of the route of administration (Fig. 5) and the type of neutral lipid (DOPE, Egg PC, and DOPC) in the galactosylated liposomes (Fig. 6). These differences between siRNA and plasmid DNA are unclear, and this event may be caused by a different mechanism in the cell between the RNAi effect

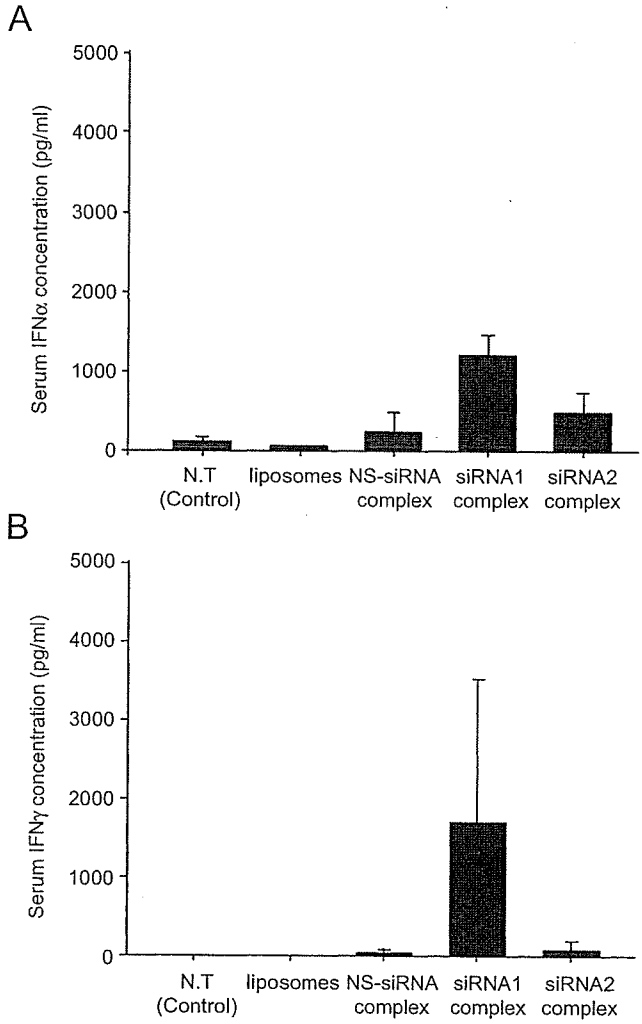

Fig. 7. Serum IFN-α (A) and IFN-γ (B) concentrations after intravenous administration of galactosylated liposomes/siRNA complex in mice. Groups of three mice were intravenously injected with galactosylated liposomes (Gal-C4-Chol/DOPE) complexed with NS-siRNA, siRNA1 and siRNA2 (5 nmol siRNA/mouse), respectively. At 5 h following administration, blood samples were collected and INF-α levels measured by ELISA. N.T. represents non-treated mice.

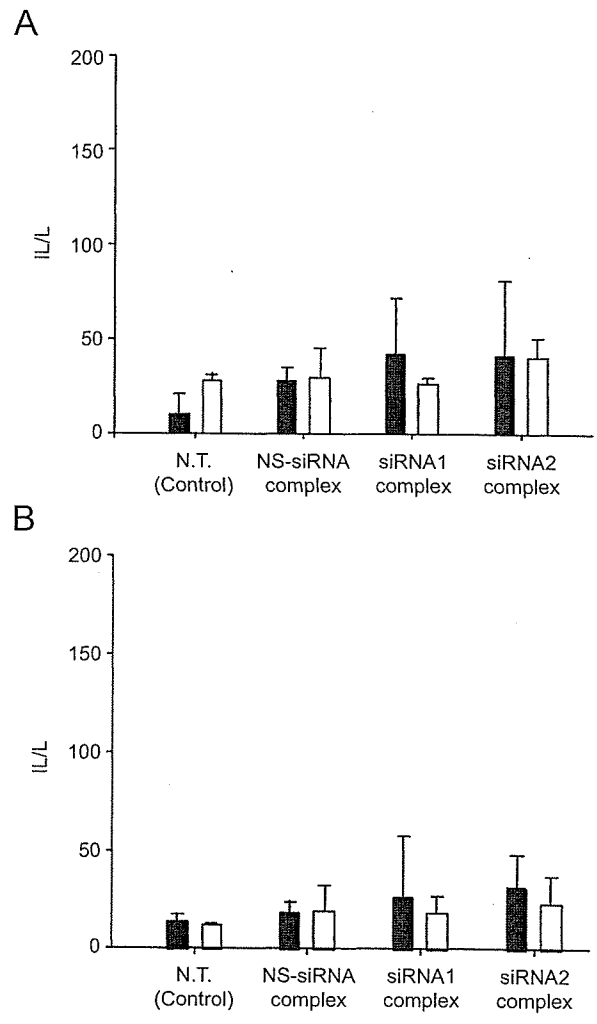

Fig. 8. Serum ALT (A) and AST (B) levels after intravenous administration of galactosylated liposomes/siRNA complex. Groups of three mice were intravenously injected with galactosylated liposomes (Gal-C4-Chol/DOPE) complexed with NS-siRNA, siRNA1 and siRNA2 (5 nmol siRNA/mouse), respectively. Blood samples were collected at 5 (black bar) and 20 h (white bar) following administration and AST and ALT levels were measured. One IU of enzyme activity represents 1 μmol substrate per 1 min at 25 °C.

by siRNA and the gene expression by plasmid DNA. This might be due to the difference in the mean diameters of the galactosylated liposomes/siRNA complex (about 75 nm) and the galactosylated lipoplex (about 100–150 nm), because we previously demonstrated that the mean diameters of galactosylated lipoplex markedly affected the transfection efficacy in PC in vivo [10].

There are three problems involved in the delivery of plasmid DNA into the cell nucleus from outside the cell and obtaining gene expression in the nucleus: the first involves approaching the cell membrane, the second involves escaping from the endosomes and the third is the passage through the membrane of the nucleus. In the case of siRNA delivery, since RNAi systems operate in cytoplasm, only two steps are needed. Moreover, siRNA has a low molecular weight and a low effective concentration in cells, compared with plasmid DNA. The characteristics of siRNA involve enhanced potential as a delivery system of galactosylated liposomes which might make it easier to design an siRNA delivery system.

It is known that IFN responses are induced by single- and double-stranded RNA associated with viral infection in mammalian cells and when siRNA is transfected into cells it is also able to stimulate type I IFN-α [24]. Furthermore, siRNA complexed with cationic liposomes containing cationic lipids (DOTAP; 1,2-dioleyl-3-trimetyl-ammoniumpropane) activates siRNA-mediated type I and II IFN responses in mice [11]. To develop an siRNA hepatocyte-selective delivery system without side-effects, it is important to avoid the immune responses. Therefore, we

evaluated the levels of IFN-α and IFN-γ, as types I and II IFN responses, in mouse serum to investigate the toxicity of the galactosylated liposomes/siRNA complex. As shown in Fig. 7, the galactosylated liposomes/siRNA complex induced IFN-α and IFN-γ depending on the sequence of siRNA when given intravenously to mice. This is consistent with recent reports about siRNA/cationic liposomes complex [18–20]. These observations lead us to believe that IFN-γ induction by galactosylated liposomes/siRNA complex can be control by optimization of the siRNA sequence. Combination therapy using IFN-γ and IFN-α and gene silencing by siRNA would be more effective for the treatment of some viral diseases i.e., hepatitis C. Therefore, further studies are needed to analyze the relationship between IFNs induction and the sequence of siRNA for designing rational treatments involving the injection of galactosylated liposomes/siRNA complex.

As shown in Fig. 8, none of the galactosylated liposomes/siRNA complexes cause significant hepatitis in mice even although the galactosylated liposomes/siRNA1 complex induced IFN-γ. It has been reported that intravenous injection of cationic liposomes/plasmid DNA complex induces hepatic toxicity [25–27]. However, the hepatic toxicity due to cationic liposomes/plasmid DNA complex is induced by proinflammatory cytokines secreted from macrophages following recognition of the CpG motif in plasmid DNA [21]. In contrast, in the case of siRNA systems, IFN responses can be controlled by optimization of the siRNA sequence (Fig. 7). Therefore, these observations suggest that siRNA may be safer than plasmid DNA when delivered by (galactosylated) cationic liposomes.

Recently, Morrissey et al. [22] reported the sustained circulation in the blood of a formulation of chemically modified siRNA employing polyethylene glycol (PEG)-modified liposomes. They demonstrated that lipid-encapsulated siRNA against HBV (hepatitis B virus) was efficiently delivered to mouse liver and reduced the HBV DNA titer in vivo. Also, it has been reported that siRNA can silence the disease target apolipoprotein B (ApoB) in the liver when administered systemically to non-human primates (cynomolgus monkeys) with PEG-modified liposomes [23]. Other reports have also described that siRNA complexed with liposomes induces RNAi effects in liver [28,29]. However, hepatocyte-selective targeting delivery systems for siRNA have not been reported yet. We suggest that the use of galactosylated liposomes for siRNA delivery is more effective in lowering the dose and increasing the effect of siRNA against HBV and apoB. Therefore, galactosylated liposomes have great potential as a therapeutic application of siRNA for the treatment of liver diseases without significant side-effects following intravenous administration.

5. Conclusion

Our results showed that siRNA could be delivered to PC in experiments involving biodistribution and cellular localization in liver with galactosylated liposomes but not with cationic liposomes when administrated via the tail vein of mice. Furthermore, we confirmed that endogenous hepatic gene (Ubc13 gene) mRNA is markedly reduced in the liver, by more than 60%, when the galactosylated liposomes/siRNA (Ubc13–siRNA) complex is used. By the optimization of RNA sequences of the galactosylated liposomes/siRNA complexes, type I IFN responses, which are induced by single- and double-stranded RNA associated with viral infection in mammalian cells, can be induced and/or controlled. In addition, the galactosylated liposomes/siRNA complex did not cause any significant hepatitis via cytokine production in mice. These observations suggest that galactosylated liposomes are an efficient carrier of siRNA for hepatocyte-selective gene silencing following intravenous administration.

Acknowledgments

This work was supported in part by Grants-in-aid for Scientific Research from the Ministry of Education, Culture, Sports, Science, and Technology of Japan, and by Health and Labour Sciences Research Grants for Research on Advanced Medical Technology from the Ministry of Health, Labour and Welfare of Japan.

References

[1] Dorsett Y, Tuschl T. siRNAs: applications in functional genomics and potential as therapeutics. Nat Rev Drug Discov 2004;3(4):318–29.
[2] Lu PY, Xie FY, Woodle MC. siRNA-mediated antitumorigenesis for drug target validation and therapeutics. Curr Opin Mol Ther 2003;5(3):225–34.
[3] Ichim TE, Li M, Qian H, Popov IA, Rycerz K, Zheng X, et al. RNA interference: a potent tool for gene-specific therapeutics. Am J Transplant 2004;4(8):1227–36.
[4] Karagiannis TC, El-Osta A. RNA interference and potential therapeutic applications of short interfering RNAs. Cancer Gene Ther 2005;12(10):787–95.
[5] Ryther RC, Flynt AS, Phillips 3rd JA, Patton JG. siRNA therapeutics: big potential from small RNAs. Gene Ther 2005;12(1):5–11.
[6] Kawakami S, Yamashita F, Nishida K, Nakamura J, Hashida M. Glycosylated cationic liposomes for cell-selective gene delivery. Crit Rev Ther Drug Carrier Syst 2002;19(2):171–90.
[7] Kawakami S, Fumoto S, Nishikawa M, Yamashita F, Hashida M. In vivo gene delivery to the liver using galactosylated cationic liposomes. Pharm Res 2000;17(3):306–13.
[8] Fumoto S, Kawakami S, Ito Y, Shigeta K, Yamashita F, Hashida M. Enhanced hepatocyte-selective in vivo gene expression by stabilized galactosylated liposome/plasmid DNA complex using sodium chloride for complex formation. Mol Ther 2004;10(4):719–29.
[9] Fumoto S, Kawakami S, Shigeta K, Higuchi Y, Yamashita F, Hashida M. Interaction with blood components plays a crucial role in asialoglycoprotein receptor-mediated in vivo gene transfer by galactosylated lipoplex. J Pharmacol Exp Ther 2005;315(2):484–93.
[10] Higuchi Y, Kawakami S, Fumoto S, Yamashita F, Hashida M. Effect of the particle size of galactosylated lipoplex on hepatocyte-selective gene transfection after intraportal administration. Biol Pharm Bull 2006;29(7):1521–3.

[11] Ma Z, Li J, He F, Wilson A, Pitt B, Li S. Cationic lipids enhance siRNA-mediated interferon response in mice. Biochem Biophys Res Commun 2005;330(3):755–9.
[12] Zhang T, Lin RT, Li Y, Douglas SD, Maxcey C, Ho C, et al. Hepatitis C virus inhibits intracellular interferon alpha expression in human hepatic cell lines. Hepatology 2005;42(4):819–27.
[13] Wang Y, Kato N, Jazag A, Dharel N, Otsuka M, Taniguchi H, et al. Hepatitis C virus core protein is a potent inhibitor of RNA silencing-based antiviral response. Gastroenterology 2006;130(3):883–92.
[14] Kawakami S, Yamashita F, Nishikawa M, Takakura Y, Hashida M. Asialoglycoprotein receptor-mediated gene transfer using novel galactosylated cationic liposomes. Biochem Biophys Res Commun 1998;252(1):78–83.
[15] Liu F, Song Y, Liu D. Hydrodynamics-based transfection in animals by systemic administration of plasmid DNA. Gene Ther 1999;6(7): 1258–66.
[16] Song E, Lee SK, Wang J, Ince N, Ouyang N, Min J, et al. RNA interference targeting Fas protects mice from fulminant hepatitis. Nat Med 2003;9(3):347–51.
[17] Matsui Y, Kobayashi N, Nishikawa M, Takakura Y. Sequence-specific suppression of mdr1a/1b expression in mice via RNA interference. Pharm Res 2005;22(12):2091–8.
[18] Hornung V, Guenthner-Biller M, Bourquin C, Ablasser A, Schlee M, Uematsu S, et al. Sequence-specific potent induction of IFN-α by short interfering RNA in plasmacytoid dendritic cells through TLR7. Nat Med 2005;11(3):263–70.
[19] Judge AD Sood V, Shaw JR, Fang D, McClintock K, MacLachlan I. Sequence-dependent stimulation of the mammalian innate immune response by synthetic siRNA. Nat Biotechnol 2005;23(4):457–62.
[20] Sioud M. Induction of inflammatory cytokines and interferon responses by double-stranded and single-stranded siRNAs is sequence-dependent and requires endosomal localization. J Mol Biol 2005;348(5):1079–90.
[21] Yew NS, Zhao H, Wu IH, Song A, Tousignant JD, Przybylska M, et al. Reduced inflammatory response to plasmid DNA vectors by elimination and inhibition of immunostimulatory CpG motifs. Mol Ther 2000;1(3):255–62.
[22] Morrissey DV, Lockridge JA, Shaw L, Blanchard K, Jensen K, Breen W, et al. Potent and persistent in vivo anti-HBV activity of chemically modified siRNAs. Nat Biotechnol 2005;23(8):1002–7.
[23] Zimmermann TS, Lee AC, Akinc A, Bramlage B, Bumcrot D, Fedoruk MN, et al. RNAi-mediated gene silencing in non-human primates. Nature 2006;441(7089):111–4.
[24] Kim DH, Longo M, Han Y, Lundberg P, Cantin E, Rossi JJ. Interferon induction by siRNAs and ssRNAs synthesized by phage polymerase. Nat Biotechnol 2004;22(3):321–5.
[25] Tousignant JD, Gates AL, Ingram LA, Johnson CL, Nietupski JB, Cheng SH, et al. Comprehensive analysis of the acute toxicities induced by systemic administration of cationic lipid: plasmid DNA complexes in mice. Hum Gene Ther 2000;11(18): 2493–513.
[26] Kawakami S, Ito Y, Charoensit P, Yamashita F, Hashida M. Evaluation of proinflammatory cytokine production induced by linear and branched polyethylenimine/plasmid DNA complexes in mice. J Pharmacol Exp Ther 2006;317(3):1382–90.
[27] Loisel S, Le Gall C, Doucet L, Ferec C, Floch V. Contribution of plasmid DNA to hepatotoxicity after systemic administration of lipoplexes. Hum Gene Ther 2001;12(6):685–96.
[28] Sorensen DR, Leirdal M, Sioud M. Gene silencing by systemic delivery of synthetic siRNAs in adult mice. J Mol Biol 2003;327(4): 761–6.
[29] Khoury M, Louis-Plence P, Escriou V, Noel D, Largeau C, Cantos C, et al. Efficient new cationic liposome formulation for systemic delivery of small interfering RNA silencing tumor necrosis factor alpha in experimental arthritis. Arthritis Rheum 2006;54(6): 1867–77.

Available online at www.sciencedirect.com
ScienceDirect
Journal of Controlled Release 116 (2006) 330–336
journal of controlled release
www.elsevier.com/locate/jconrel

PEGylated lysine dendrimers for tumor-selective targeting after intravenous injection in tumor-bearing mice

Tatsuya Okuda [a,b], Shigeru Kawakami [a], Naomi Akimoto [a], Takuro Niidome [c], Fumiyoshi Yamashita [a], Mitsuru Hashida [a,*]

[a] *Department of Drug Delivery Research, Graduate School of Pharmaceutical Sciences, Kyoto University, 46-29 Yoshida-Shimoadachi-cho, Sakyo-ku, Kyoto 606-8501, Japan*
[b] *Japan Association for the Advancement of Medical Equipment, 3-42-6 Hongo, Bunkyo-ku, Tokyo113-0033, Japan*
[c] *Department of Applied Chemistry, Faculty of Engineering, Kyushu University, 744 Motooka, Nishi-ku, Fukuoka 819-0395, Japan*

Received 11 August 2006; accepted 25 September 2006
Available online 30 September 2006

Abstract

In this study, we synthesized a sixth generation lysine dendrimer (KG6) and two PEGylated derivatives thereof and evaluated their biodistribution characteristics in both normal and tumor-bearing mice. The intact KG6 showed a rapid clearance from the blood stream and non-specific accumulation in the liver and kidney. In contrast, the PEGylated derivatives showed a better retention in blood and low accumulativeness in organs dependent of the rate of PEGylation. In addition, PEGylated KG6 with a high modification rate was accumulated effectively in tumor tissue via the enhanced permeability and retention (EPR) effect. Moreover, we clarified that multiple administrations did not affect the biodistribution characteristics of a second dose of PEGylated KG6. PEGylated lysine dendrimer would be a useful material for a clinically applicable tumor-targeting carrier.

Keywords: Drug carrier; EPR effect; Lysine dendrimers; PEGylation; Tumor targeting

1. Introduction

Augmenting the drug concentration in tumor tissue with high selectivity is the most worthwhile subject of current cancer chemotherapy using macromolecular drug formulations. Although almost all anti-cancer drugs are pharmacologically active, the clinical application of these drugs is limited due to low solubility, unfavorable biodistribution characteristics, and serious side effects. Therefore, improving their disadvantageous biodistribution is important not only to reduce toxicity but also to boost the therapeutic effect of anti-cancer drugs. It has been reported that, the modification of a biocompatible polymer, polyethylene glycol (PEG), can extend retention time in blood by decreasing non-specific interactions with endogenous components and macrophages. For instance, Doxil® is a representative commercialized PEGylated liposomal formulation of doxorubicin [1]. In this formulation, a PEGylated liposome, i.e. STEALTH® liposome, enhances therapeutic effect and decreases serious side effects such as cardiotoxicity of doxorubicin by improving its biodistribution [2]. Furthermore, it has been reported that macromolecules having long blood retention and ~200 nm in size, such as PEGylated liposomal or polymeric formulations, effectively accumulate into the solid tumor tissue via the enhanced permeability and retention (EPR) effect. However, small and narrow sized drug carriers would be certain to be delivered to even small sized tumors by the EPR effect.

One candidate for a small and narrow sized drug carrier is a dendrimer, but little information is available on the tumor-selective disposition of (PEGylated) dendrimers after intravenous administration. Recently, dendritic polymers like polyamidoamine (PAMAM) dendrimer, which is a typical dendrimer, have attracted great attention in terms of biomedical

* Corresponding author. Fax: +81 75 753 4575.
E-mail address: hashidam@pharm.kyoto-u.ac.jp (M. Hashida).

0168-3659/$ - see front matter © 2006 Elsevier B.V. All rights reserved.
doi:10.1016/j.jconrel.2006.09.012

applications [3,4]. Although the PAMAM dendrimer has already been tested as a carrier for drugs and genes and as a contrast agent for bioimaging [5–10], it has been reported to be cytotoxic [11]. In order to construct a highly safe carrier molecule, we designed a lysine dendrimer taking into consideration the safety of the constituent unit, and employed L-lysines as branch units. We have developed a sixth generation of lysine dendrimer (KG6), which produces highly branched dendritic polymers [12]. Indeed, lysine dendrimers showed no significant cytotoxicity in cultured cells compared with PAMAM dendrimer [12]. Since lysine dendrimers have many reactive primary amino groups derived from the α- and ε-amino groups of the L-lysine residue on their surface [13], they can be modified by several functional groups. More recently, we have evaluated the disposition characteristics of lysine dendrimers and PEGylated KG6 and demonstrated that most of lysine dendrimers were accumulated in the liver, but PEGylated KG6 was sustained in the blood after intravenous administration in mice [14]. These observations prompted us to investigate whether PEGylated KG6 could be delivered to tumors selectively in tumor-bearing mice.

In this study, the physicochemical properties of PEGylated KG6 derivatives were evaluated. After the radiolabeling with [^{111}In] of PEGylated KG6 derivatives, the disposition characteristics were analyzed in tumor-bearing mice after intravenous administration. The effect of administration number of PEGylated KG6 derivatives was also evaluated for clinical use.

2. Materials and methods

2.1. Chemicals

Di-*t*-butyl dicarbonate (Boc_2O) was purchased from Peptide Institute, Inc. (Osaka, Japan). The organic solvents used for synthesis, lysine monohydrochloride, and hexamethylenediamine were obtained from Wako Pure Chemical Industries, Ltd. (Osaka, Japan). Trifluoroacetic acid, dicyclohexyl amine (DCHA), and triethylamine were purchased from Nacalai Tesque, Inc. (Kyoto, Japan). The coupling reagents, 2-(*1H*-benzotriazole-1-yl)-1,1,3,3-tetramethyluronium hexafluorophosphate (HBTU) and 1-hydroxybenzotriazol (HOBt) were acquired from Novabiochem, Merk Ltd. (Tokyo, Japan). The DTPA anhydride was purchased from Dojindo (Kumamoto, Japan). The $^{111}InCl_3$ was kindly provided by Nihon Medi-Physics Co. Ltd. (Hyogo, Japan).

2.2. Synthesis of lysine dendrimers and conjugation with DTPA

Lysine monohydrochloride was dissolved in distilled water, and a 2.2 M equivalent of Boc_2O in dioxane was added. The pH of the reaction mixture was adjusted to 8.0 or higher with 1 M NaOH. After overnight stirring at room temperature, dioxane was evaporated and the product was extracted to ethylacetate. The organic phase was washed three times with 10% citric acid and saturated NaCl, respectively, and then evaporated. *N*-Boc protected lysine was crystallized by petroleum ether with an equivalent molar ratio of DCHA. Lysine dendrimers were synthesized according to a method reported previously [12]. In brief, for the first generation synthesis, the 2.2 M excess of *N*-Boc protected lysines were coupled with hexamethylenediamine in DMF by the HBTU–HOBt method [15], and then, de-protection was achieved with TFA treatment. For the 2nd and higher generations, the coupling reaction between the amino group-free previous generation of dendrimers and *N*-Boc protected lysines was performed in DMF by the HBTU–HOBt method, and subsequently Boc-groups were removed by TFA. We synthesized lysine dendrimers up to the sixth generation by repeating these coupling and de-protection procedures. Then KG6 was conjugated with DTPA in order to radiolabel it with ^{111}In [16]. In brief, KG6 was dissolved in 20 mM borate buffer (pH 9.8) and DTPA anhydride in dimethyl sulfoxide was added at the molar ratio of 1:1. After 1 h of mixing at room temperature, the reaction mixture was purified by ultrafiltration using VIVASPIN-20 (MWCO 5,000). The purified DTPA-labeled KG6 was then lyophilized.

2.3. PEGylation of KG6

In order to prevent steric hindrance by PEG chains on the surface of the dendrimer, the DTPA-labeled KG6 was used for PEGylation. The DTPA-labeled KG6 was dissolved in borate buffer (pH 9.8) and reacted with PEG-NHS (Mw: 5,000) at 4 °C. After an overnight incubation, the reaction mixture was ultrafiltrated using VIVASPIN (MWCO 100,000). The purified PEGylated KG6 was then lyophilized. The modification rate of surface primary amino groups by PEG-NHS was evaluated by the barium–iodine method [17].

2.4. Evaluation of physicochemical properties of KG6 and its PEGylated derivatives

KG6 and its PEGylated derivatives were dissolved in PBS (pH 7.3) at a concentration of up to 5 mg/ml, and then their particle size and zeta-potential were measured with a Zetasizer Nano ZS (Malvern Instruments Ltd., United Kingdom).

2.5. Radiolabeling of dendrimers

For the biodistribution experiments, each dendrimer was radiolabeled with ^{111}In via DTPA, according to the method of Hnatowich et al. [16]. This radiolabeling method is suitable for examining the biodistribution of macromolecules from plasma to various tissues, because radioactive metabolites, if produced after cellular uptake, are retained within cells where the uptake takes place [18,19]. A DTPA-labeled dendrimer solution dissolved in a 100 mM sodium citrate buffer (pH 5.5) at a concentration of 2 mg/ml was prepared. Twenty microliters of $^{111}InCl_3$ solution was mixed with equivalent volume of 100 mM sodium citrate buffer, and the mixture was stood for a few minutes. Forty microliters of DTPA-labeled dendrimer solution was then added and mixed well. After standing for 30 min at room temperature, the mixture was purified by gel filtration chromatography using a PD-10 column and eluted with sodium citrate buffer (pH 5.5). The appropriate fractions were selected based on their radioactivity and concentrated by ultrafiltration using VIVASPIN-20.

2.6. Animals

Male ddY mice (5 weeks old, 25–27 g) were purchased from Shizuoka Agricultural Co-operative Association for Laboratory Animals, Shizuoka, Japan. For preparation of the tumor-bearing model, male CDF1 mice (4 weeks old) were purchased from the company mentioned above, and 1×10^6 cells of colon 26 were subcutaneously inoculated into the back of CDF1 mice. Then the mice were kept until the tumor had reached about 100 mm^3 in volume. Tumor volume is calculated as follows: volume$=1/2\times LW^2$ (L is the long diameter and W is the short diameter of a tumor). Animals were maintained under conventional housing conditions. All experiments with animals were performed according to the Guidelines for Animal Experimentation at Kyoto University.

2.7. Biodistribution experiments

The biodistribution experiments in both normal and tumor-bearing mice were performed according to the following method. ^{111}In-labeled dendrimer was dissolved in saline, and the concentration of dendrimer was adjusted by addition of non-radiolabeled dendrimer to the solution. The ^{111}In-labeled dendrimer solution was administrated intravenously via the tail at a dose of 1 mg/kg. At an appropriate time after the intravenous injection, blood was collected from the vena cava under ether anesthesia and the mice were sacrificed. The liver, kidneys, spleen, heart, and lungs were removed, rinsed with saline, blotted dry, and weighed. The collected blood was centrifuged for 5 min at 2000 ×g to prepare a plasma sample. The collected organs and 100 μl of plasma were transferred into a counting tube, and the radioactivity of each sample was measured using a gamma counter.

For the biodistribution experiments, in which the effect of multiple injections of PEGylated KG6 on the biodistribution characteristics of the second dose was investigated, the first dose was injected 5 days before the second dose, because it has been reported that the ABC phenomenon occurred most effectively at 5 days post-injection of the first dose [20]. In this experiment, non-radiolabeled intact KG6 and PEG(76)-KG6 were used as the first dose at a concentration of 0.1 mg dendrimer/kg and 1 mg dendrimer/kg. Then, 1 mg dendrimer/kg of PEG(76)-KG6 including the radiolabeled one was administered to mice via the tail vein at 5 days after the first dose. All subsequent procedures were performed according to the method described above.

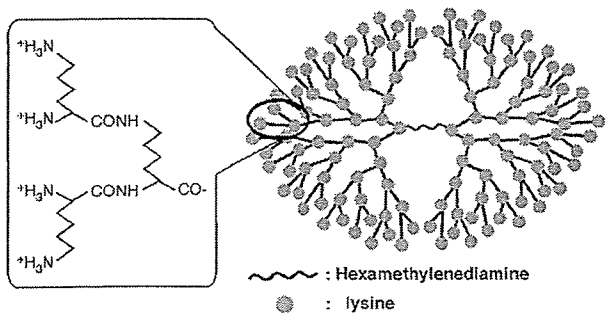

Fig. 1. Structure of the sixth generation dendritic poly(L-lysine) (KG6).

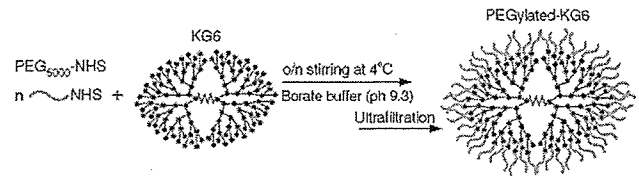

Scheme 1. Schematic presentation of the procedure used to synthesize PEGylated KG6.

2.8. Statistical analysis

Statistic analysis was performed using Student's paired t-test for two groups. Multiple comparisons among different generations were made with the Tukey–Kramer test. $P<0.05$ was considered to be indicative of statistical significance.

3. Results

3.1. Synthesis of PEGylated KG6

The structure of the sixth generation lysine dendrimer (KG6) is shown in Fig. 1. In accordance with a method described previously, KG6 was synthesized using the hexamethylenediamine as the initiator core. The coupling and de-protection steps were performed with a yield of about 75–98%. In the next step, KG6 was reacted with an equivalent molar ratio of DTPA anhydride. Then, PEGylated KG6 was synthesized according to Scheme 1. The PEGylation was performed at two different molar ratios. As a result of quantification of the introduced PEG chain by the barium–iodine method [17], two PEGylated KG6 derivatives having different modification rates have been synthesized. The numbers of introduced PEG chains were 10 and 76.1 per KG6 molecule (Table 1). We call these derivatives PEG(10)-KG6 and PEG(76)-KG6, respectively.

3.2. Physicochemical properties of PEGylated KG6 derivatives

The physicochemical properties of PEGylated KG6 derivatives were analyzed by Zetasizer Nano ZS (Table 1). The mean diameter of PEG(10)-KG6 was slightly larger (about 7.75 nm) than that of intact KG6 (about 5.85 nm), while the particle size

Table 1
Physicochemical properties of PEGylated KG6 in PBS

	No. of PEG_{5000}[a]	No. of $-NH_2$ groups[b]	Particle size (nm)	Zeta-potential (mV)
KG6	0	128	5.85±0.06	19.77±0.30
PEG(10)-KG6	10	118	7.75±0.70	0.00±0.03
PEG(76)-KG6	76.2	51.8	16.92±0.13	−6.51±0.18

Each value represents the mean±SD of three experiments.
[a] The number of PEG_{5000} was determined by the barium–iodine method.
[b] The number of surface amino groups was determined by subtracting the result of the barium–iodine method from the number of native KG6's surface amino groups.

of PEG(76)-KG6 was much larger (about 16.9 nm). Although the zeta-potential of intact KG6 was positive, both PEGylated derivatives had an almost neutral zeta-potential.

3.3. Plasma concentration of ^{111}In-labeled PEGylated KG6 derivatives

Fig. 2 shows the short-term (A) and long-term (B) plasma concentration profiles of ^{111}In-labeled PEGylated KG6 derivatives after intravenous injection into mice. Although the intact KG6 was rapidly eliminated from the circulation within a few minutes, the retention of PEGylated KG6 derivatives was enhanced by modification with PEG chains (Fig. 2A). This enhancing effect was acquired even by introducing ten PEG chains. However, as the modification rate increased, so too did the amount of PEGylated KG6 retained in the blood stream. In the case of PEG(76)-KG6, about 20% of the injected dose was still circulating in the blood stream (Fig. 2B).

3.4. Tissue distribution of ^{111}In-labeled PEGylated KG6 derivatives

The biodistribution characteristics of PEGylated KG6 derivatives and intact KG6 were evaluated until 60 min post-intravenous injection into mice by measuring the radioactivity in the organs and urine. The dendrimers were almost undetectable in the spleen, heart, lung, and urine (data not shown).

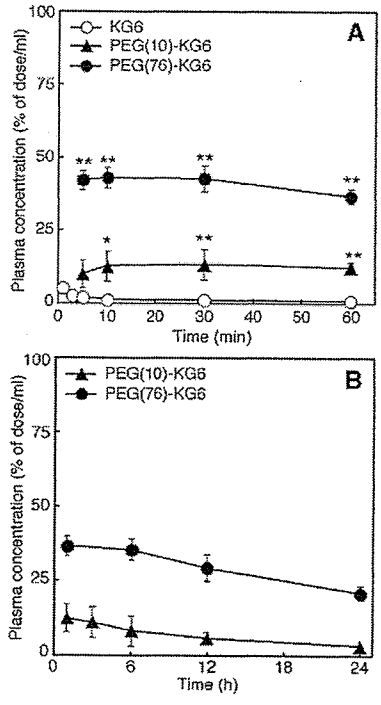

Fig. 2. The short-term (A) and long-term (B) plasma concentration profiles of ^{111}In-labeled PEGylated KG6 after intravenous administration to mice at a dose of 1 mg/kg. Each value represents the mean±SD of three experiments. The intact KG6 (○), PEG(10)-KG6 (▲), and PEG(76)-KG6 (●) were subjected to biodistribution experiments. Statistically significant differences (*, $P<0.05$; **, $P<0.01$) between PEGylated KG6 and intact KG6 at each time point.

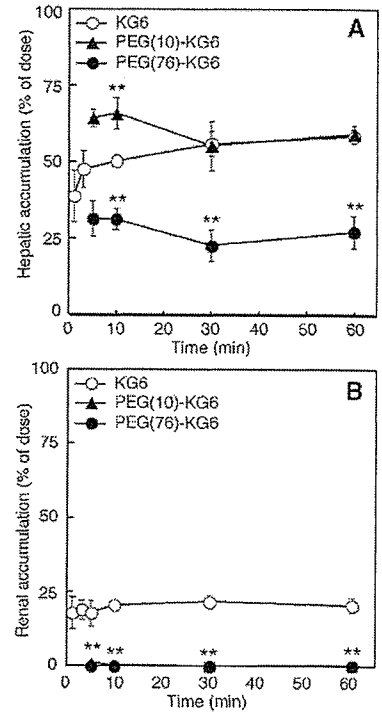

Fig. 3. Hepatic (A) and renal (B) accumulation of ^{111}In-labeled PEGylated KG6 after intravenous administration to mice at a dose of 1 mg/kg. The intact KG6 (○), PEG(10)-KG6 (▲), and PEG(76)-KG6 (●) were subjected to biodistribution experiments. Each value represents the mean±SD of three experiments. Statistically significant differences (*, $P<0.05$; **, $P<0.01$) between PEGylated KG6 and intact KG6 at each time point.

The amount of PEG(10)-KG6 accumulated in the liver was the almost same as that of intact KG6 (Fig. 3A). In contrast, the accumulation of PEG(76)-KG6 in liver was fairly suppressed (Fig. 3A). On the other hand, the renal accumulation of intact KG6 was observed, whereas no detectable levels of radioactivity derived from PEGylated KG6 derivatives were detected from the kidneys (Fig. 3B).

3.5. Tumor accumulation of PEG(76)-KG6 in the tumor-bearing model mice

In order to clarify whether the intravenously injected PEGylated KG6 accumulated into the solid tumor tissue or not, a biodistribution analysis of PEG(76)-KG6 which showed a more advantageous blood retention was performed in tumor-bearing mice (Fig. 4). In the case of intact KG6, no significant accumulation was observed in the tumor at any time point. In contrast, PEG(76)-KG6 gradually accumulated into the tumor. The tumor accumulation rate of PEG(76)-KG6 reached 14.6% of dose/g tumor, whereas that of intact KG6 was only 2.2% of dose/g tumor even at 24 h post-injection.

3.6. Plasma concentration of ^{111}In-labeled PEGylated KG6 after multiple injections

In order to confirm whether the first dose of dendrimers (intact or PEGylated KG6) affect the biodistribution characteristics of the

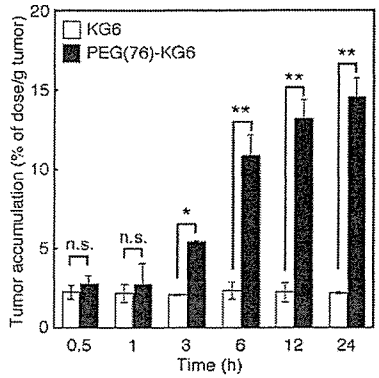

Fig. 4. Time-dependent tumor accumulation of ^{111}In-labeled PEG(76)-KG6 after intravenous administration to CT26 tumor-bearing CDF1 mice at a dose of 1 mg/kg. Each value represents the mean±SD of three experiments. Closed and open bars represent tumor accumulation of PEG(76)-KG6 and intact KG6, respectively. Statistically significant differences (*, $P<0.05$; **, $P<0.01$) between PEG(76)-KG6 and intact KG6 at each time point.

second dose of PEG(76)-KG6, pre-injection of the dendrimers was performed at 5 days before the biodistribution analysis of the second dose of PEG(76)-KG6. We used 0.1 mg/kg and 1 mg/kg of intact KG6 or PEG(76)-KG6 as the first dose of dendrimers. In addition, we used saline treatment as a control. The blood concentration profiles of the second dose of intravenously administered PEG(76)-KG6 are shown in Fig. 5. As shown in Fig. 5A and B, no significant changes in blood concentration

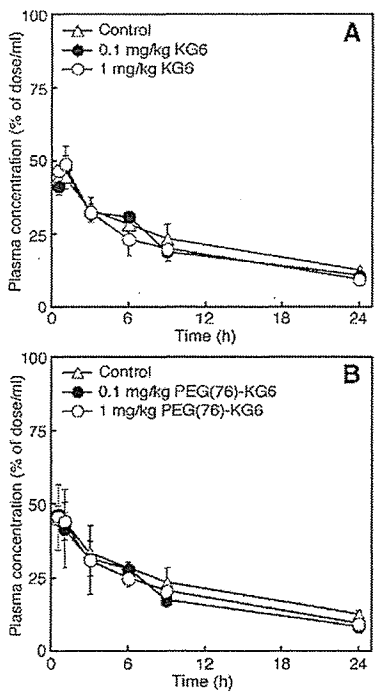

Fig. 5. Plasma concentration profiles of ^{111}In-labeled PEG(76)-KG6 after intravenous administration in intact KG6 (A) or PEG(76)-KG6 (B) pretreated mice. Each value represents the mean±SD of three experiments. The mice were pretreated with intact KG6 or PEG(76)-KG6 at a concentration of 0.1 mg/kg (●) and 1 mg/kg (○). The saline pretreatment was used as a control (△). Subsequently, ^{111}In-labeled PEG(76)-KG6 was intravenously administered at day 5 post-first injection.

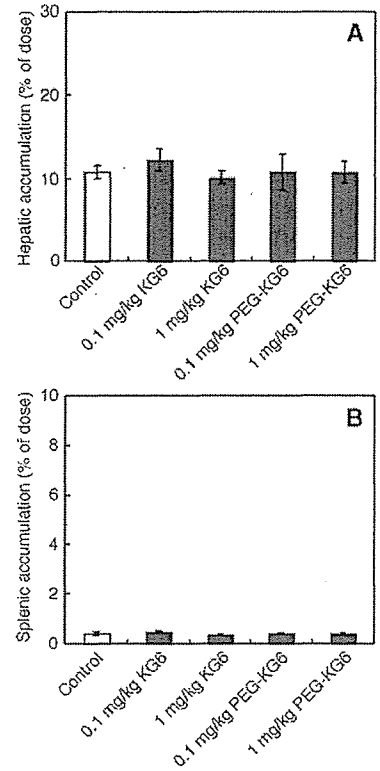

Fig. 6. Hepatic (A) and splenic (B) accumulation of ^{111}In-labeled PEG(76)-KG6 in intact KG6 or PEG(76)-KG6 pretreated mice at 24 h post-injection. The saline pretreatment was used as a control. Each value represents the mean±SD of three experiments.

profiles of the second dose of PEG(76)-KG6 were observed even if the concentration and formulation of the first dose were different.

3.7. Hepatic and splenic accumulation of ^{111}In-labeled PEGylated KG6

Since the organs of the reticuloendothelial system (RES), such as the liver and spleen, play an important role in the metabolism and excretion of foreign substance, we evaluated the hepatic and splenic accumulation of the second dose of PEG (76)-KG6 at 24 h post-injection (Fig. 6). Both the hepatic and splenic accumulation rate were almost the same under all conditions used, though we administered two types of dendrimers at two different concentrations as the first dose.

4. Discussion

It is expected that a more functional and safer drug carrier system will be developed. We have previously reported that KG6 showed no significant toxicity to cultured cells compared with the PAMAM dendrimer [12]. More recently, we have also reported that KG6 has no acute hepatic toxicity and the PEGylation of KG6 caused a sustained retention of KG6 in the blood stream [14]. Therefore, in this study, we employed KG6 as a candidate base molecule for a tumor-targeting drug carrier that is highly safe, and

evaluated the physicochemical properties and biodistribution characteristics of intact and PEGylated KG6.

The synthesis of lysine dendrimers up to the sixth generation could be achieved with good yields, and then, the PEGylation of KG6 was performed in accordance with the method described in Scheme 1. As a result of the quantification of the PEGylation rate, two PEGylated KG6 derivatives the modification rate of which is about 7.8% (PEG(10)-KG6) and 59.4% (PEG(76)-KG6), respectively, were synthesized (Table 1). The particle size of intact KG6 was about 5.85 nm, whereas that of PEG(10)-KG and PEG(76)-KG6 was about 7.75 nm and 16.92 nm, respectively (Table 1). Both PEG(10)-KG6 and PEG(76)-KG6 showed almost a neutral zeta-potential, while the zeta-potential of intact KG6 was positive (Table 1). These increments in size and changes of zeta-potential from positive to neutral suggest that PEGylation of KG6 was certainly achieved. Since the polymeric micelles and liposomes are assemblies of many molecules, the reproducibility may be low. The hyperbranched polymers that have many branches like dendrimers are not assemblies, but they are usually a mixture of many polymer molecules with irregular structure and size. Hence, the reproducibility of this type of polymer may be also not good. The linear poly-L-lysines also consist of lysines. However, almost of all commercially available linear poly-L-lysine is a mixture of molecules with various molecular weight due to their synthetic procedure. Though linear poly-L-lysine can be synthesized as uniform molecules by solid phase synthesis, mass production is very difficult. In contrast to these compounds, the lysine dendrimer can be mass-produced as a monodispersed molecule not an assembly; accordingly its reproducibility would be better than that of polymeric micelles, liposomes and hyperbranched polymers. In addition, dendrimers are smaller in size than polymeric micelles and liposomes. Therefore the use of dendrimers as drug carriers probably enables one to achieve a more precise and effective drug targeting.

In order to evaluate biodistribution of the characteristics of intact and PEGylated KG6, these dendrimers were radiolabeled with [^{111}In] and injected into mice. Intravenously administered intact KG6 was rapidly eliminated from the circulation within few minutes (Fig. 2A). This rapid elimination is probably due to accumulation in the liver and kidney in the early phase (Fig. 3). However, PEGylation of KG6 enhances the retention in blood, and this effect is boosted as the PEGylation rate is increased (Fig. 2A). However, PEG(10)-KG6 accumulated in the liver at almost the same level as intact KG6, whereas the hepatic accumulation of PEG(76)-KG6 was slightly suppressed (Fig. 3A). In addition, PEGylation of KG6 resulted in no renal accumulation (Fig. 3B). As these results show, the non-specific interaction with biomolecules and non-specific accumulation in organs via electrostatic interaction is suppressed by modification with PEG chains. Consequently, the retention of PEGylated KG6 derivatives in the blood stream was enhanced.

To investigate whether the PEGylated KG6 shows tumor tissue accumulativeness, PEG(76)-KG6, which showed a better blood retention, was radiolabeled and was also subjected to tumor-bearing mice. As shown in Fig. 4, although the intact KG6 hardly showed tumor accumulativeness, PEG(76)-KG6 gradually and effectively accumulated in tumor tissue. Maeda and Matsumura reported that macromolecules ~200 nm in size and with a prolonged retention in blood extravasate into the interstitial space of solid tumors through the poorly constructed tumoral vascular wall and stay there because tumors usually lack effective lymphatic drainage; consequently, they accumulate in tumor tissue effectively by the EPR effect [21]. Since PEG(76)-KG6 fulfills the requirement of blood retention and size for causing the EPR effect (Table 1 and Fig. 2), PEG(76)-KG6 probably accumulated in the tumor tissue via this effect. This result is well consistent with that of polymeric micelles having a PEG moiety and PEGylated liposomes [22–26]. These results suggest that PEGylation is applicable to dendrimeric molecules like lysine dendrimers for tumor targeting.

As far as the actual clinical use of drug formulations is concerned, multiple administrations are frequently performed. It has been reported that multiple injections of PEGylated liposomes induce an accelerated blood clearance (ABC) phenomenon on the second injection [27]. Therefore, the induction of the ABC phenomenon may be an obstacle to therapy. Hence, we evaluated the effect of multiple administrations on the biodistribution characteristics of the second dose of PEGylated KG6. As shown in Fig. 5, the blood concentration profile of the second dose of PEG(76)-KG6 was unchanged regardless of the composition and concentration of pre-injected dendrimers. Moreover, in the case of PEGylated liposomes, it has been reported that the ABC phenomenon was probably due to uptake by the reticuloendothelial system (RES) particularly in the liver [28]. However, no significant increase in hepatic or splenic accumulation was observed under any conditions we tested (Fig. 6). These results suggest that PEGylated KG6 would become a multi-administrable drug carrier molecule.

The following two methods would be available for drug loading to PEGylated lysine dendrimer: 1) covalent bonding via surface primary amine groups, 2) non-covalent drug incorporation into the inner space of lysine dendrimer taking advantage of the physicochemical interaction such as hydrophobic interaction. In the case of covalent bonding, the drugs would be stably bonded to the dendrimer, but the drugs must have functional group to form a covalent bond with primary amino groups of lysine dendrimer and the appropriate device to release the drugs at target site may be needed. Furthermore, it is necessary to consider the loss of amino groups by conjugation of PEG chains and the steric hindrance of introduced PEG chains. In contrast, in the case of non-covalent incorporation of drugs, no peculiar functional groups or devices are required. In this case, however, the alteration of inner structure of dendrimer may be needed to hold the drugs stably. Moreover, the size and structural feature would be restricted because the inner space of lysine dendrimer is limited. Probably, about up to 1000 in molecular weight is acceptable and the planar structure such as anti-cancer drugs is suitable. Although the appropriate drug loading method should be selected, the non-covalent incorporation would be more suitable as a drug loading method for PEGylated lysine dendrimer.

In conclusion, we synthesized KG6 and two PEGylated derivatives thereof and evaluated their biodistribution characteristics